THE DESCRIPTIVE AND DYNAMIC OCEANOGRAPHY OF THE MESOSTRUCTURE NEAR ARCTIC ICE MARGINS.

Allan Eugene Karrer

NAVAL POSTGRADUATE SCHOOL
Monterey, California

THESIS

THE DESCRIPTIVE AND DYNAMIC
OCEANOGRAPHY OF THE MESOSTRUCTURE
NEAR ARCTIC ICE MARGINS

by

Allan Eugene Karrer

September 1975

Thesis Advisor: R. G. Paquette

SECURITY CLASSIFICATION OF THIS PAGE (When Data Entered)

REPORT DOCUMENTATION PAGE		READ INSTRUCTIONS BEFORE COMPLETING FORM
1. REPORT NUMBER	2. GOVT ACCESSION NO.	3. RECIPIENT'S CATALOG NUMBER
4. TITLE (and Subtitle) The Descriptive and Dynamic Oceanography of the Mesostructure near Arctic Ice Margins		5. TYPE OF REPORT & PERIOD COVERED Master's Thesis; September 1975 6. PERFORMING ORG. REPORT NUMBER
7. AUTHOR(s) Allan Eugene Karrer		8. CONTRACT OR GRANT NUMBER(s)
9. PERFORMING ORGANIZATION NAME AND ADDRESS Naval Postgraduate School Monterey, California 93940		10. PROGRAM ELEMENT, PROJECT, TASK AREA & WORK UNIT NUMBERS ZS52-555-001 62759N
11. CONTROLLING OFFICE NAME AND ADDRESS Naval Postgraduate School Monterey, California 93940		12. REPORT DATE September 1975 13. NUMBER OF PAGES 91
14. MONITORING AGENCY NAME & ADDRESS(if different from Controlling Office) Naval Postgraduate School Monterey, California 93940		15. SECURITY CLASS. (of this report) Unclassified 15a. DECLASSIFICATION/DOWNGRADING SCHEDULE

16. DISTRIBUTION STATEMENT (of this Report)

Approved for public release; distribution unlimited

17. DISTRIBUTION STATEMENT (of the abstract entered in Block 20, if different from Report)

18. SUPPLEMENTARY NOTES

19. KEY WORDS (Continue on reverse side if necessary and identify by block number)

Mesostructure; Microstructure; Arctic; Chukchi Sea; MIZPAC; Oceanography; Sound Velocity; Sea Ice

20. ABSTRACT (Continue on reverse side if necessary and identify by block number)

Complex temperature anomalies observed near Arctic ice margins in the Chukchi Sea were found to be associated with the interaction of the warm coastal current with the ice cover and resident bottom water. These anomalies were characterized by large temperature gradients found in areas of very low density gradient. They were in the form of inversions, interleavings, and discrete parcels which

DD FORM 1 JAN 73 1473 EDITION OF 1 NOV 65 IS OBSOLETE
S/N 0102-014-6601 |
(Page 1)

varied greatly in short distances. The processes which produced mesostructure were directly linked to the presence of ice and were found to affect the entire water column. Structure was found in the vicinity of the ice margin but was observed to dissipate well inside the ice margin. A dynamic high was found which was related to the melting of ice and characteristically occurred in the melting zone of the ice margin. This dynamic high was limited to a depth of 10 meters and is believed to be a factor in the deepening of mesostructure elements and other phenomena as they pass the ice margin with the current.

The Descriptive and Dynamic Oceanography of the Mesostructure near Arctic Ice Margins

by

Allan Eugene Karrer
Lieutenant, United States Navy
B.S., Drexel Institute of Technology, 1968

Submitted in partial fulfillment of the
requirements for the degree of

MASTER OF SCIENCE IN OCEANOGRAPHY

from the

NAVAL POSTGRADUATE SCHOOL
September 1975

ABSTRACT

Complex temperature anomalies observed near Arctic ice margins in the Chukchi Sea were found to be associated with the interaction of the warm coastal current with the ice cover and resident bottom water. These anomalies were characterized by large temperature gradients found in areas of very low density gradient. They were in the form of inversions, interleavings, and discrete parcels which varied greatly in short distances. The processes which produced mesostructure were directly linked to the presence of ice and were found to affect the entire water column. Structure was found in the vicinity of the ice margin but was observed to dissipate well inside the ice margin. A dynamic high was found which was related to the melting of ice and characteristically occurred in the melting zone of the ice margin. This dynamic high was limited to a depth of 10 meters and is believed to be a factor in the deepening of mesostructure elements and other phenomena as they pass the ice margin with the current.

TABLE OF CONTENTS

I. INTRODUCTION - 10

A. DESCRIPTION OF THE PROBLEM - - - - - - - - - - - 10

B. DATA BACKGROUND AND SOURCE - - - - - - - - - - - 10

C. DESCRIPTION OF THE MIZPAC 74 AREA- - - - - - - - 14

D. OBJECT OF THE STUDY- - - - - - - - - - - - - - - 15

II. INVESTIGATIONAL PROCEDURE- - - - - - - - - - - - - 16

III. DISCUSSION - 17

A. TEMPERATURE CHARACTERISTICS- - - - - - - - - - 17

B. DENSITY CHARACTERISTICS- - - - - - - - - - - - 36

C. HEAT BALANCE ACROSS AN ICE MARGIN- - - - - - - 45

D. DYNAMIC HEIGHTS AND LOCAL CURRENTS - - - - - - 52

IV. CONCLUSIONS- 64

A. SUMMARY OF RESULTS - - - - - - - - - - - - - - 64

B. RECOMMENDATIONS FOR FUTURE INVESTIGATIONS- - - 68

APPENDIX A - STD DATA FOR STATIONS ANALYZED- - - - - - - 69

BIBLIOGRAPHY - 89

INITIAL DISTRIBUTION LIST- - - - - - - - - - - - - - - - 90

LIST OF TABLES

I. Heat Excess and Ice Excess for Crossings 1 through 7 - - - - - - - - - - - - - - - - 48

II. Dynamic Heights for Crossing 1 through 7 - - - - - - 54

III. Comparison of Crossing Characteristics - - - - - - - 58

LIST OF FIGURES

1. Definition of Mesostructure Elements- - - - - - - - -11
2. Positions of Ice Margin and Crossings - - - - - - - -13
3. Temperature Profiles, Crossing 1- - - - - - - - - - -18
4. Temperature Profiles, Crossing 2- - - - - - - - - - -19
5. Temperature Profiles, Crossing 3- - - - - - - - - - -20
6A. Temperature Profiles, Crossing 4 (First Part) - - -21
6B. Temperature Profiles, Crossing 4 (Second Part)- - -22
7. Temperature Profiles, Crossing 5- - - - - - - - - - -23
8. Temperature Profiles, Crossing 6- - - - - - - - - - -24
9. Temperature Profiles, Crossing 7- - - - - - - - - - -25
10. Temperature Cross Section, Crossing 1 - - - - - - - -28
11. Temperature Cross Section, Crossing 2 - - - - - - - -29
12. Temperature Cross Section, Crossing 3 - - - - - - - -30
13. Temperature Cross Section, Crossing 4 - - - - - - - -31
14. Temperature Cross Section, Crossing 5 - - - - - - - -32
15. Temperature Cross Section, Crossing 6 - - - - - - - -33
16. Temperature Cross Section, Crossing 7 - - - - - - - -34
17. Sigma-t Cross Section, Crossing 1 - - - - - - - - - -37
18. Sigma-t Cross Section, Crossing 2 - - - - - - - - - -38
19. Sigma-t Cross Section, Crossing 3 - - - - - - - - - -39
20. Sigma-t Cross Section, Crossing 4 - - - - - - - - - -40
21. Sigma-t Cross Section, Crossing 5 - - - - - - - - - -41
22. Sigma-t Cross Section, Crossing 6 - - - - - - - - - -42
23. Sigma-t Cross Section, Crossing 7 - - - - - - - - - -43
24. Heat and Ice Melt Content for Crossing 2- - - - - - -49

25. Dynamic Heights at 0, 5, 10, and 40 Meter Depths for Crossing 2 - - - - - - - - - - - - - - - - - 55

26. Effect of the Dynamic Hill on the Current Profile - 60

27. Effect of Eddy Viscosity on Current Velocity Diminution- 62

ACKNOWLEDGEMENT

The author is especially grateful to Dr. R. G. Paquette of the Naval Postgraduate School faculty for his patience and guidance in the preparation of this manuscript, and for his assistance in the computations. Dr. R. H. Bourke was very helpful in the calculation of the dynamic height data. My wife, Vickie, did the original typing and was untiring in providing assistance and support.

I. INTRODUCTION

A. DESCRIPTION OF THE PROBLEM

An investigation was conducted to examine the mechanisms associated with the phenomenon of temperature mesostructure found in the water columns near Arctic ice margins. The term mesostructure describes the relatively large anomalies which occur in the vertical temperature profiles; such a profile is shown in Figure 1. Corse (1974) defined an element of mesostructure as that portion of the profile from the depth where the temperature gradient became positive to the depth at which the temperature was again the value it had when the gradient became positive. These anomalies were considered as warm, vice cold, since they were found to be associated with the advection of warm water into the region. The magnitude of an element was found to be of the order of meters in depth and of tenths of degrees in temperature variation. The phenomenon of mesostructure was found to be associated with the presence of an ice margin and was present to some degree in all ice margin crossings investigated in this study.

B. DATA BACKGROUND AND SOURCE

Investigations into temperature structure near ice margins had their origin in reports of severe deterioration of sonar propagation, which was believed to be the result of complex sound-speed profiles near the ice margins. As

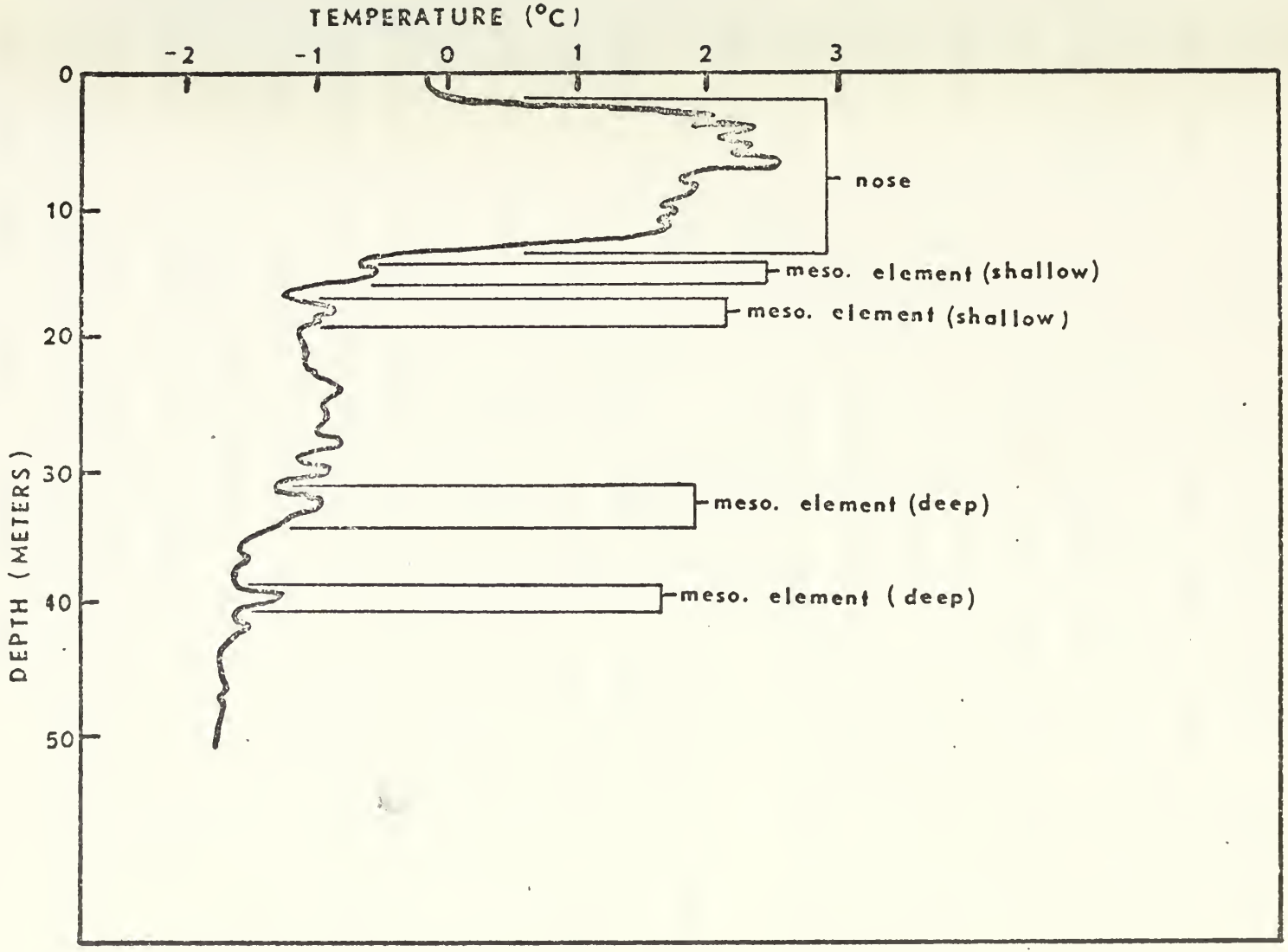

Figure 1. Definition of Mesostructure Elements.

a result of this interest, research cruises, under the general project title MIZPAC, were directed by the Arctic Submarine Laboratory, Naval Undersea Center. These cruises, carried out in 1971, 1972, and 1974 on Coast Guard ice breakers, have resulted in a data base of 350 STD stations with another such cruise scheduled for 1975. The results of the 1971 and 1972 cruises were published (Paquette and Bourke, 1973, 1974) and those for 1974 and 1975 are in preparation by Paquette and Bourke. The data from the 1974 cruise were analyzed because they were the most useful of the available data, due to the number of ice crossings and the close proximity of the stations.

The 1974 data were collected using a Bissett-Berman Model 9006 STD. Two lowerings were required for each station; a deep cast, and a shallow cast with the conductivity sensor shunted with a precision resistor to enable recording of the low salinities encountered near the surface. Seven series of closely spaced stations were analyzed, each one representing a penetration of the ice margin and termed a "crossing." Figure 2 indicates the location of the crossings, carried out during the period 18 July to 26 July 1974, and several positions of the ice margin for this period. The positions of the ice margin were derived from cruise data and NOAA-4 VHRR satellite photographs interpreted by the NOAA-NESS Environmental Products Group.

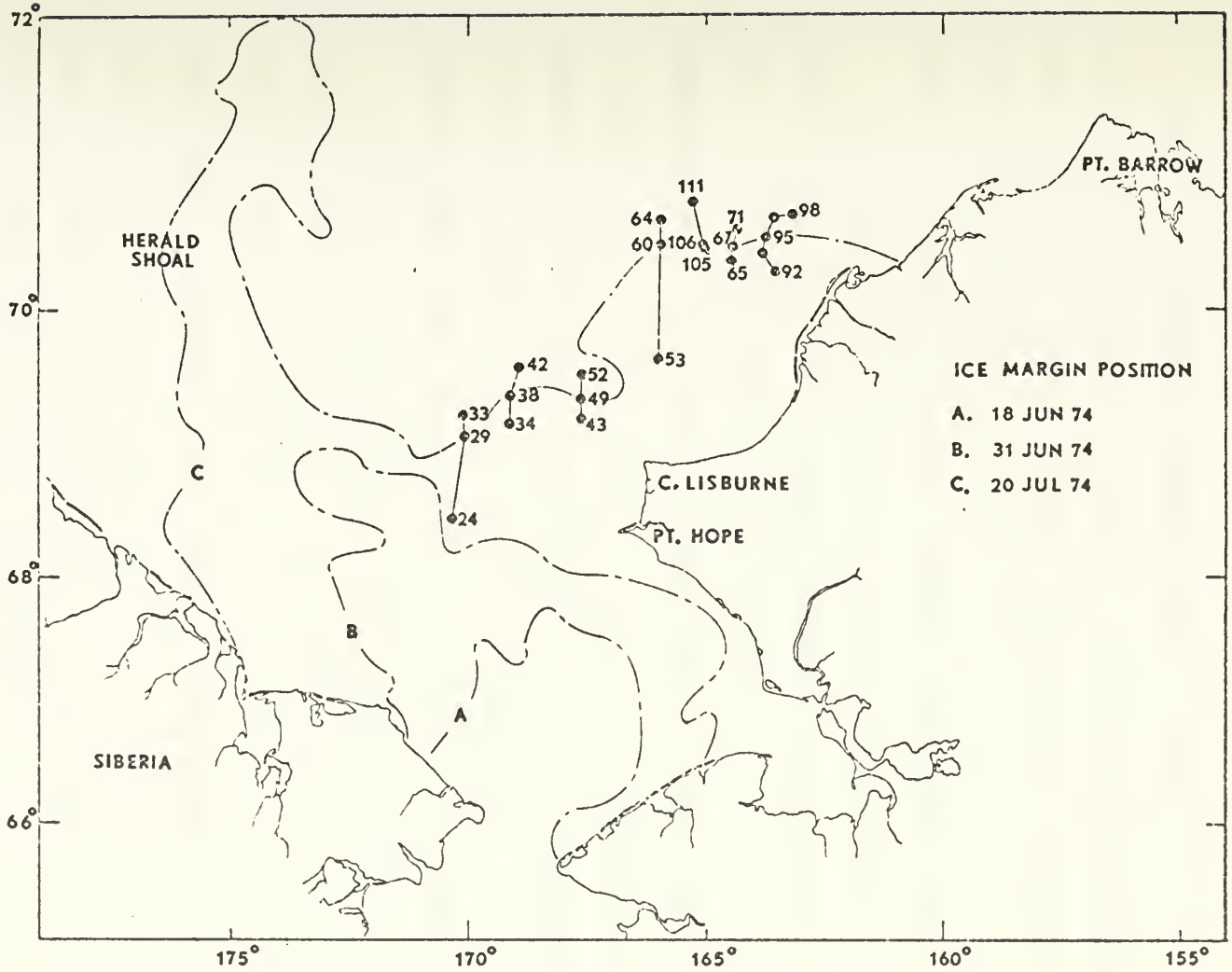

Figure 2. Location of Crossings and Ice Margin.

C. DESCRIPTION OF THE MIZPAC 74 AREA

The Chukchi Sea is a marginal sea with very little bottom relief in the area of interest and with an average depth of about 45 m.

The ice coverage and thus the ice margin varied considerably during the months of June through August 1974 (Fig. 2). There is much year-to-year variation. In 1974 the ice melted back from Bering Strait in June to 73°N by the end of August, farther north than normal.

The pattern of the melting process followed closely that of the previously known current system of the Chukchi Sea. The summer surface circulation of the Chukchi Sea is dominated by a general northward flow of warm water from Bering Strait. This flow was observed by Paquette and Bourke (1974) and was typified by a surface temperature of 5° to 11°C during late June through September and probably involved the upper mixed layer of 10 to 20 m depth. Little is known about the movement of the lower layer. The current was described as staying to the right side of the Chukchi Sea and splitting at Cape Lisburne, one branch following the Alaskan coast and the other turning north-north-west toward Herald Shoal. Garrison et a. (1973) reported the speed, relative to an ice floe, of the current along the Alaskan coast near 72°N to vary between 10 and 50 cm sec^{-1}, with a velocity shear between 10 and 20 m which was usually associated with the pynocline.

D. OBJECT OF THE STUDY

The thrust of this undertaking was to gain an understanding of the mechanisms by which mesostructure is formed, utilizing new data and previous findings. It was particularly directed toward finding the relationship between the formation of mesostructure and the following processes: the influx of warm water and the melting of the ice cover, the sloping of the density surfaces, the dynamic heights near the ice margin, and local currents. Additionally, it was desired to determine if different processes were responsible for deep and shallow mesostructure.

II. INVESTIGATIONAL PROCEDURE

The data presentations were predicated on the assumption that warm water flowed northward toward the ice and that the interaction of ice and water resulted in mesostructure. It was expected that the phenomena involved would be evident in vertical sections of the conventional oceanographic properties along the lines of the several ice-margin crossings. Temperature and sigma-t sections were therefore prepared. The latter, being closely related to salinity at locally observed water temperatures, eliminated the need for salinity sections.

Later it became apparent that the question of direction of flow of the warm water could be investigated by means of the heat and ice melt contents of the water column. The local dynamic height gradient near the ice margin seemed a possible driving force for downward mixing. These parameters also were computed for the ice-margin crossings.

III. DISCUSSION

A. TEMPERATURE CHARACTERISTICS

The temperature profiles, nested in sequence, for each ice margin crossing are shown in Figures 3 through 9. The station number and bottom temperature (°C) are indicated at the bottom of each trace, and the ice concentration in oktas (eighths) is displayed at the top with the symbol "X" indicating no data. The station numbers increased as the ice margin was penetrated from outside the ice; thus the crossings proceeded from left to right in all figures.

The temperature profiles displayed several characteristics which were common to all the crossings in general. A layer of relatively warm water, between the surface and 20 m depth, appeared outside the ice in all cases. This layer was cooled and modified with progress toward and across the ice margin and was greatly diminished or absent well inside the ice margin. Surficial cooling caused the temperature maximum of this layer to descend several meters when ice was encountered forming the "nose" feature described by Paquette and Bourke (1973).

Corse (1974) described mesostructure as being divided into three classes: the nose feature, and shallow and deep structure. He defined shallow structure as having sigma-t values less than 25.5 and deep structure as that with greater values. He placed the sigma-t value of 25.5 at about 20 m depth; however, as will be seen, this

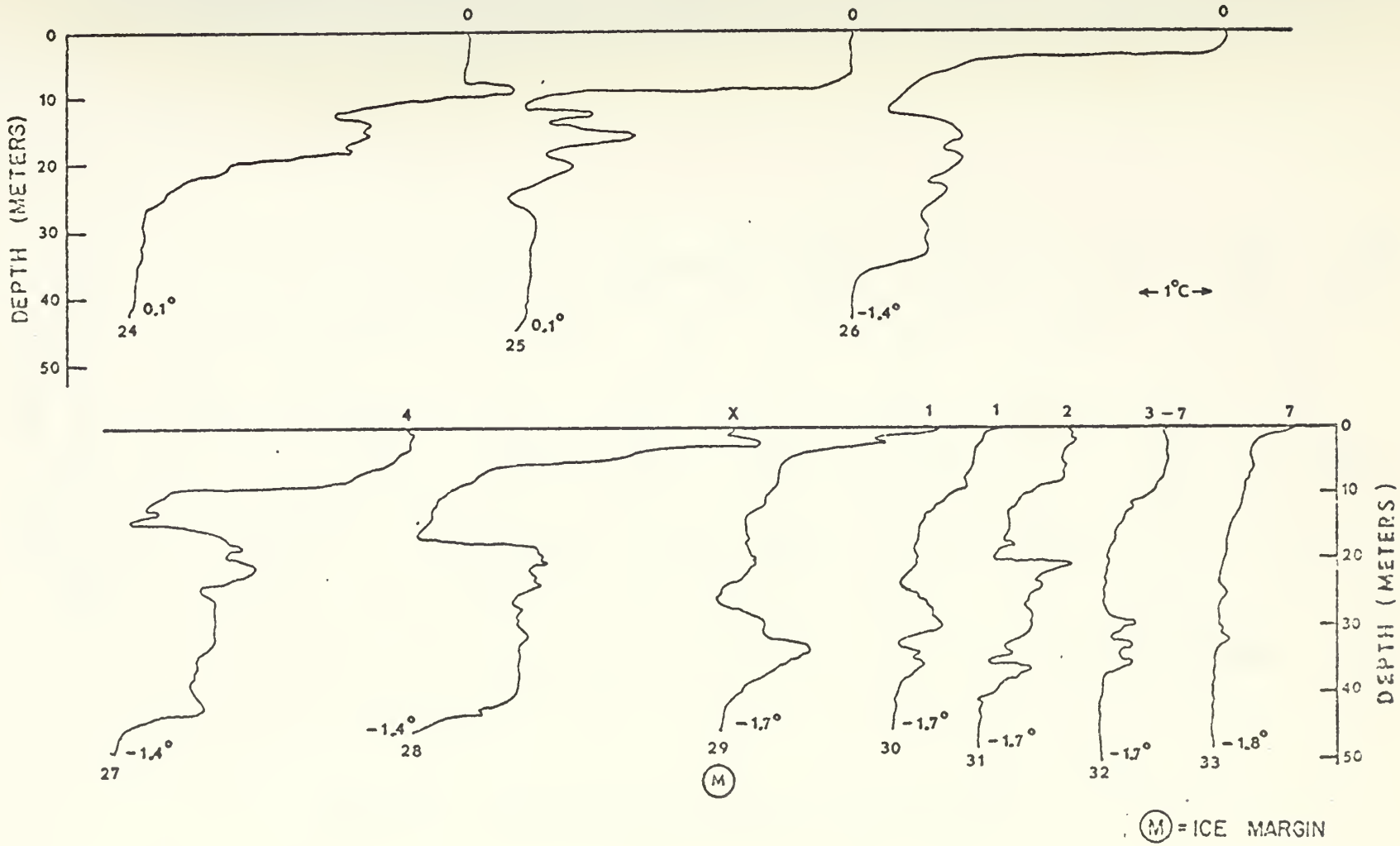

Figure 3. Temperature Profiles, Crossing 1.

Numbers at the top of trace are ice concentrations; at the bottom of the trace the bottom temperature.

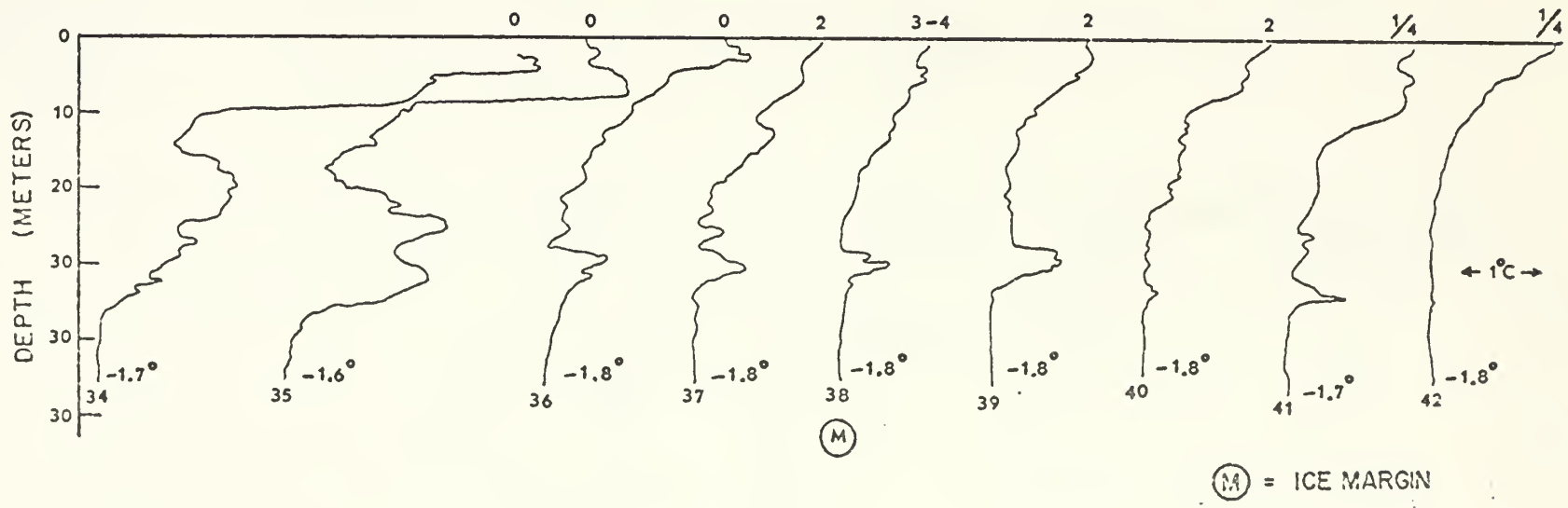

Figure 4. Temperature Profiles, Crossing 2.

Numbers at the top of trace are ice concentrations; at the bottom of the trace the bottom temperature.

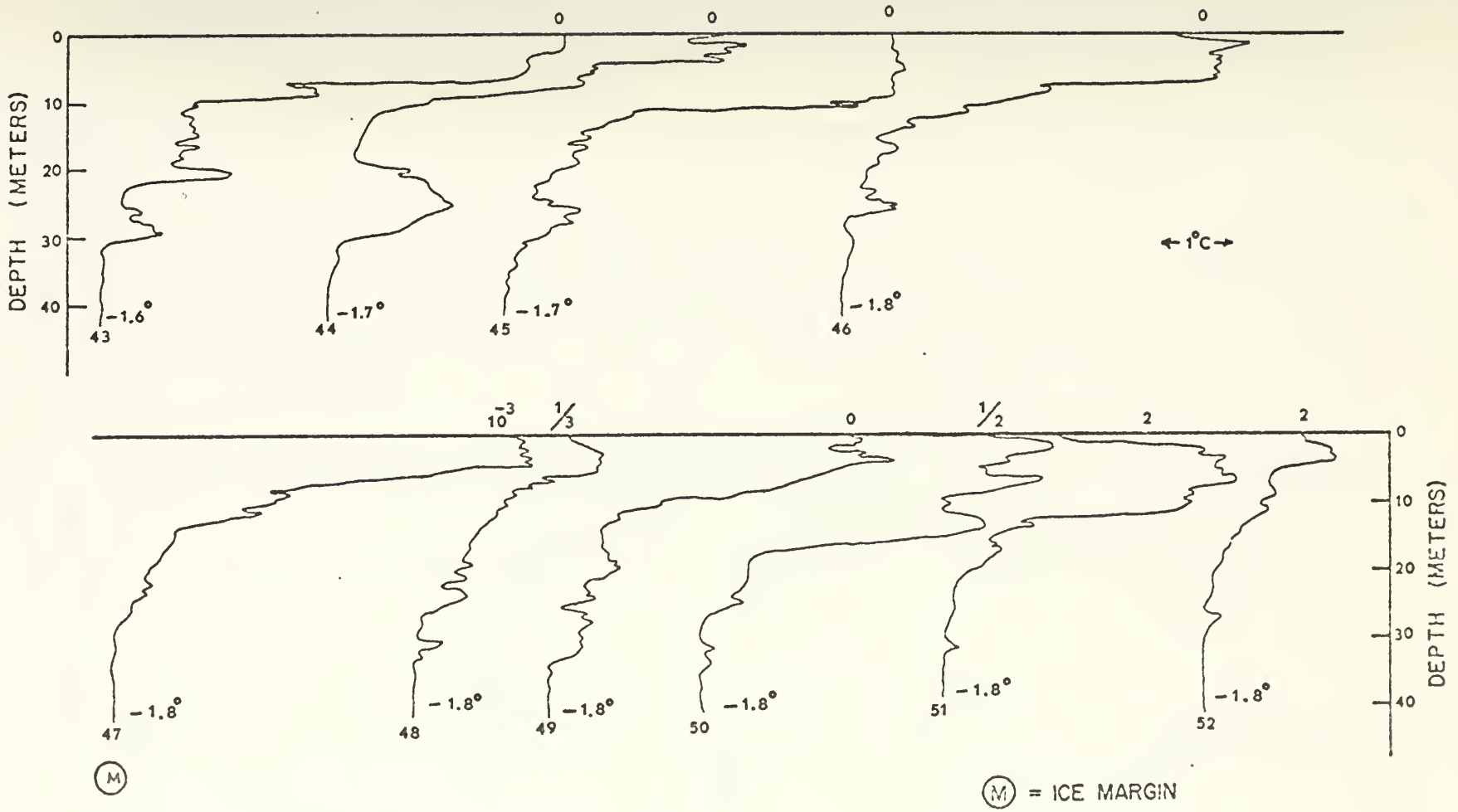

Figure 5. Temperature Profiles, Crossing 3.

Numbers at the top of trace are ice concentrations; at the bottom of the trace the bottom temperature.

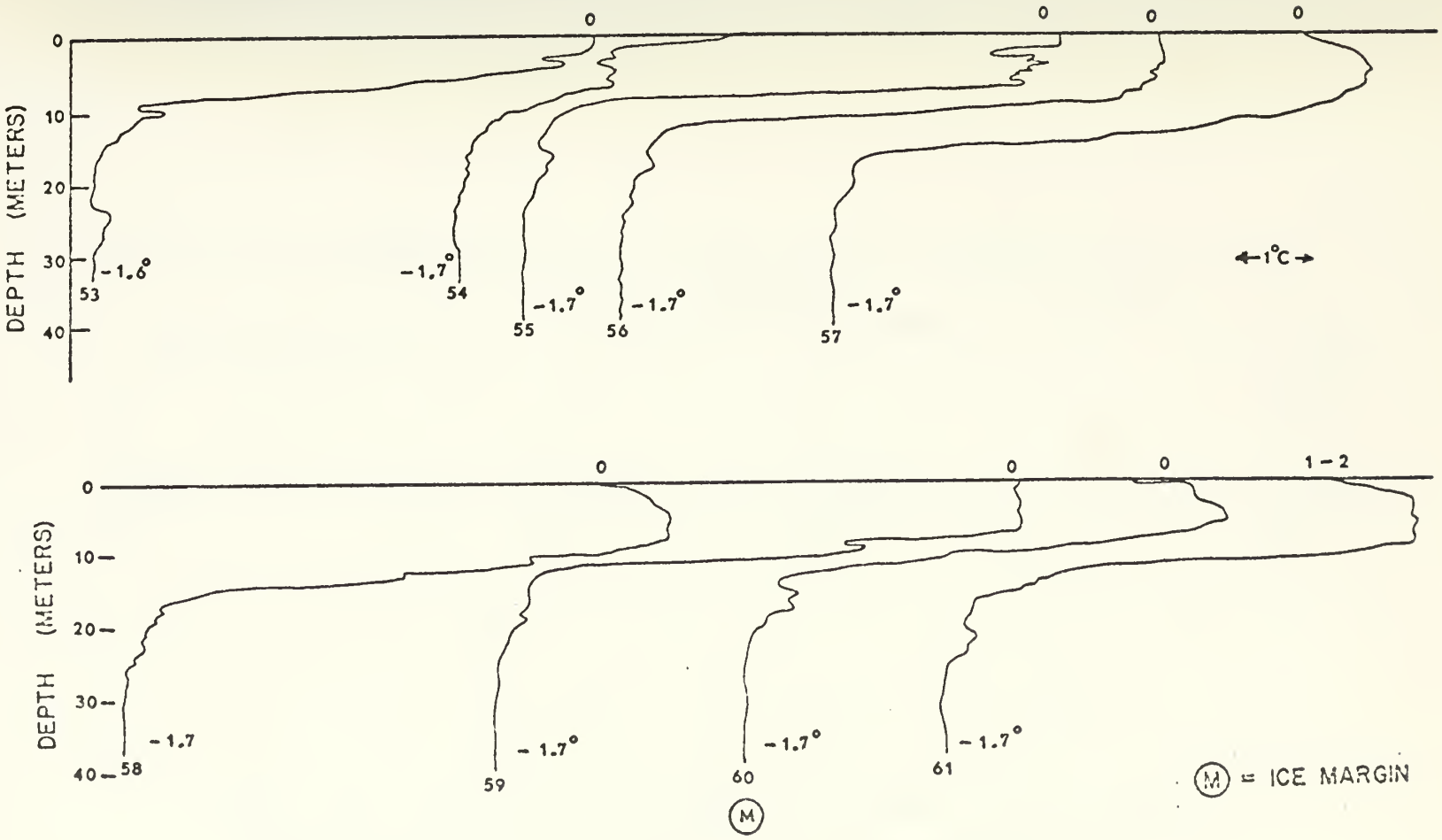

Figure 6A. Temperature Profiles, Crossing 4, First Part.

Numbers at the top of trace are ice concentrations; at the bottom of the trace the bottom temperature.

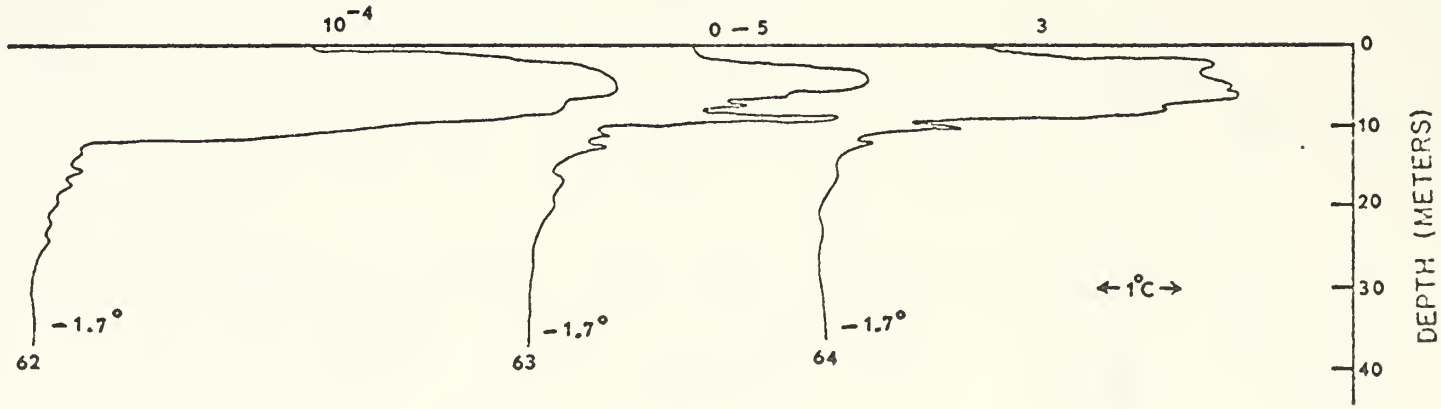

Figure 6B. Temperature Profiles, Crossing 4, Second Part.

Numbers at the top of trace are ice concentrations; at the bottom of the trace the bottom temperature.

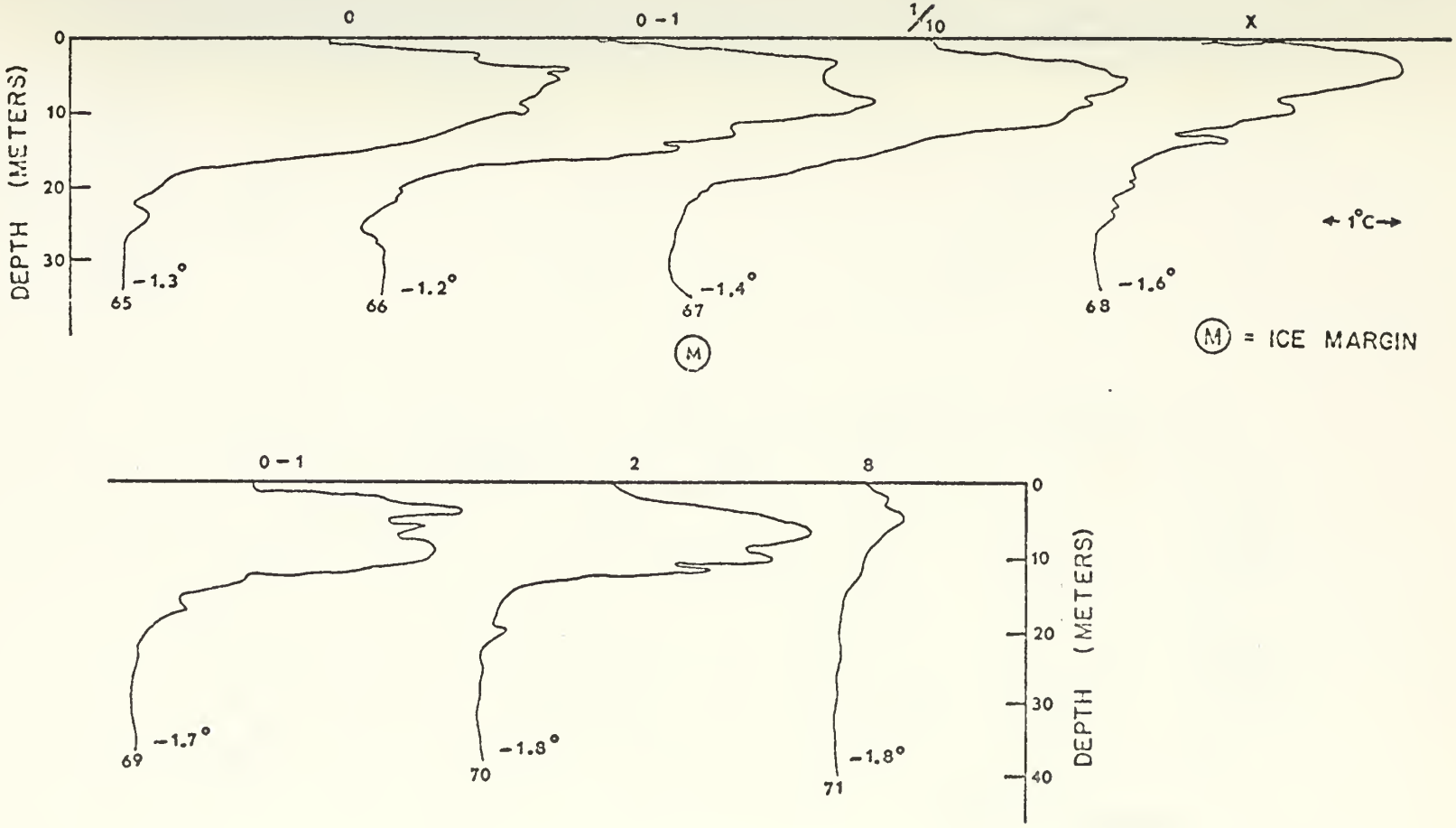

Figure 7. Temperature Profiles, Crossing 5.

Numbers at the top of trace are ice concentrations; at the bottom of the trace the bottom temperature.

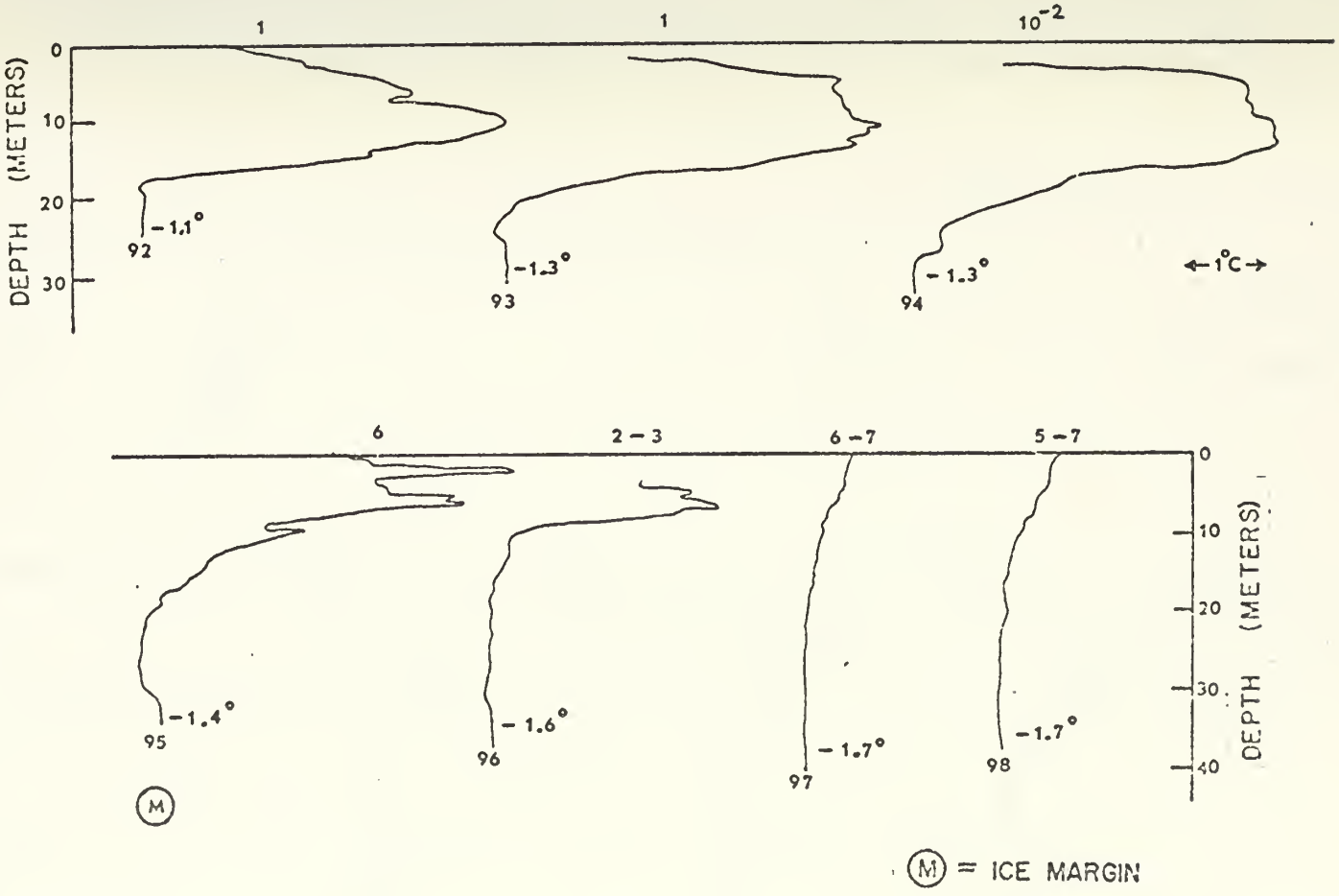

Figure 8. Temperature Profiles, Crossing 6.

Numbers at the top of trace are ice concentrations; at the bottom of the trace the bottom temperature.

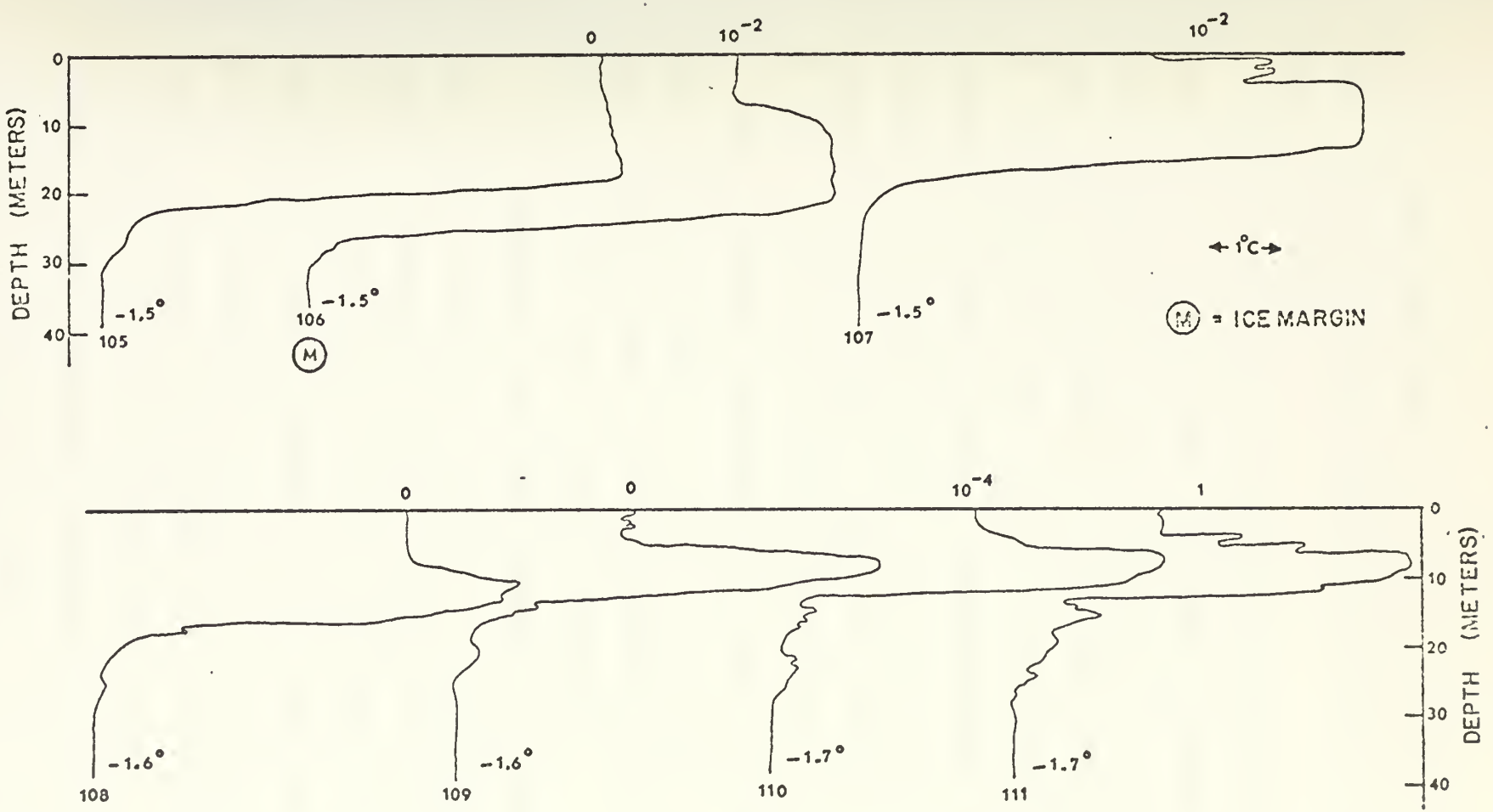

Figure 9. Temperature Profiles, Crossing 7.

Numbers at the top of trace are ice concentrations; at the bottom of the trace the bottom temperature.

investigation found the 26.0 surface at about 20 m. This depth was used to make a distinction between shallow and deep mesostructure.

Shallow structure was present in varying degrees of severity in all crossings. Crossing 3 exhibited the most severe shallow structure as compared to the lesser intensities found in Crossings 4, 5, and 6 and to Crossings 1 and 2, which displayed very little shallow structure. The presence of shallow structure correlated well with the presence of the nose feature, which was present in all crossings except 1 and 2. Thus, the nose feature appeared to have a causal relationship with shallow structure.

Deep structure was found to be severe in Crossings 1 and 2 and very slight or absent in the other crossings. The presence of deep structure appeared to be a separate phenomenon from that of shallow structure.

The temperature profiles displayed no apparent correlation between the presence of mesostructure and the maximum temperature present. This differed from the belief of Corse (1974) in the relationship between high temperatures and the presence of deep mesostructure. However, the formation and presence of structure, both shallow and deep, did correlate with the presence of an ice margin, as did the formation and descent of the nose feature. The mesostructure eventually almost disappeared at some point within the ice margin. This may indicate that the structure had been dissipated as it moved

"downstream" with a northerly flowing current past the ice edge or that there was little or no water flow toward the ice.

Vertical cross-sections of temperature for the seven crossings are presented in Figures 10 through 16. Again the relatively warm surface layer, with a maximum temperature of 3 to 6°C, may be observed south of the ice at depths of less than 20 m. This layer cooled drastically and lost most of its warmth in the vicinity of the ice margin. This was obviously due to a utilization of this heat for the melting process which will be discussed in a later section. Referring to the cross-sections, the isotherms were very irregular and displayed large gradients, many inversions, interleavings, and lenses. These irregularities were more pronounced in the vicinity of the ice margin and dissipated when well inside it, as has already been stated in the description of the profiles. Individual elements of mesostructure usually could not be traced for more than two consecutive stations, a distance of 1 to 5 km. The maximum distance over which a mesostructure feature was traced was about 11 km. This is in reasonable agreement with the results of Corse (1974). He found typical correlation distances of 1 to 2 km. Structure was found to exist for some time after the disappearance of ice from an area since it was found as far as 28 km south of the ice margin where the ice had apparently been recently.

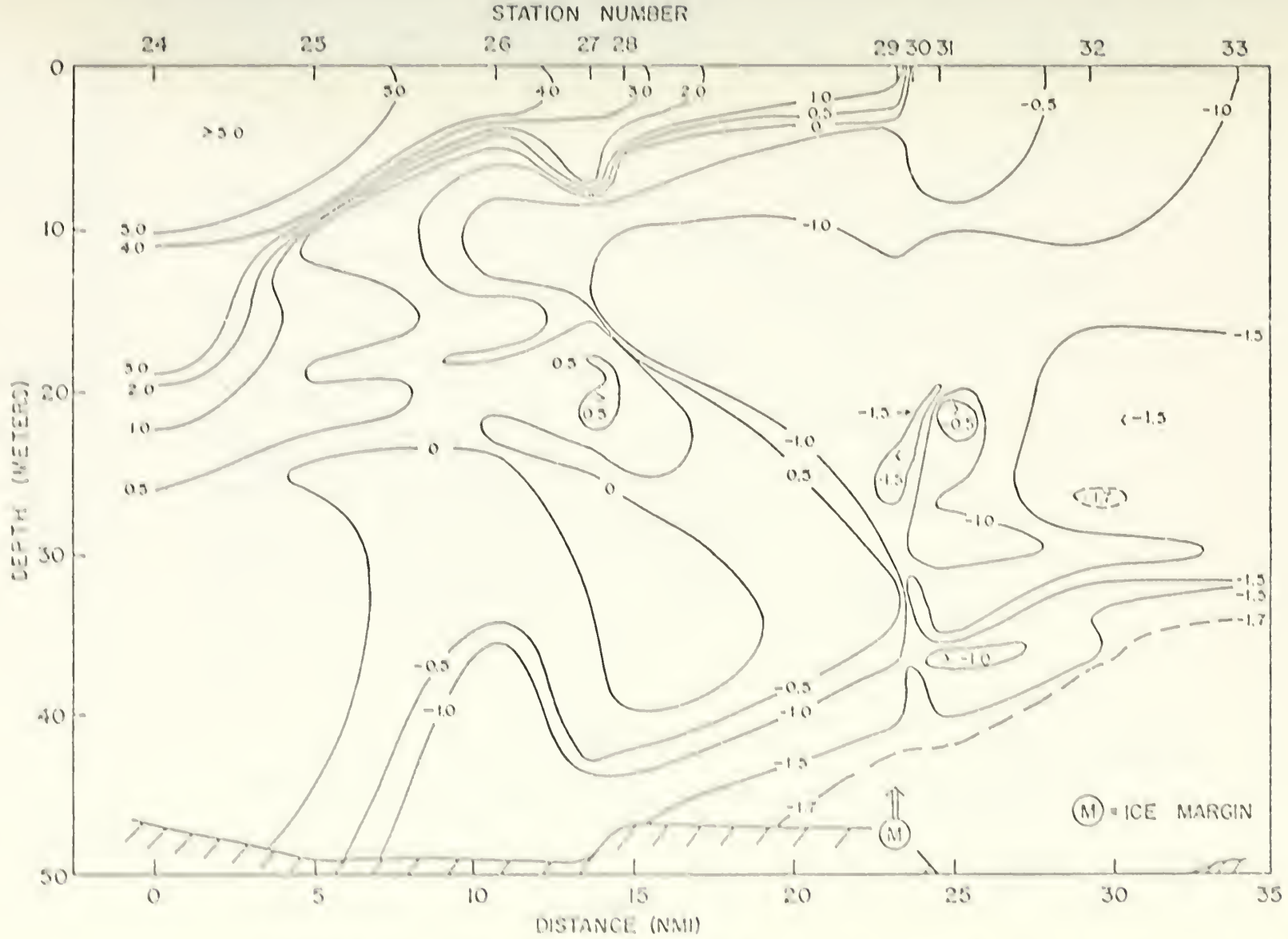

Figure 10. Temperature Cross Section, Crossing 1.

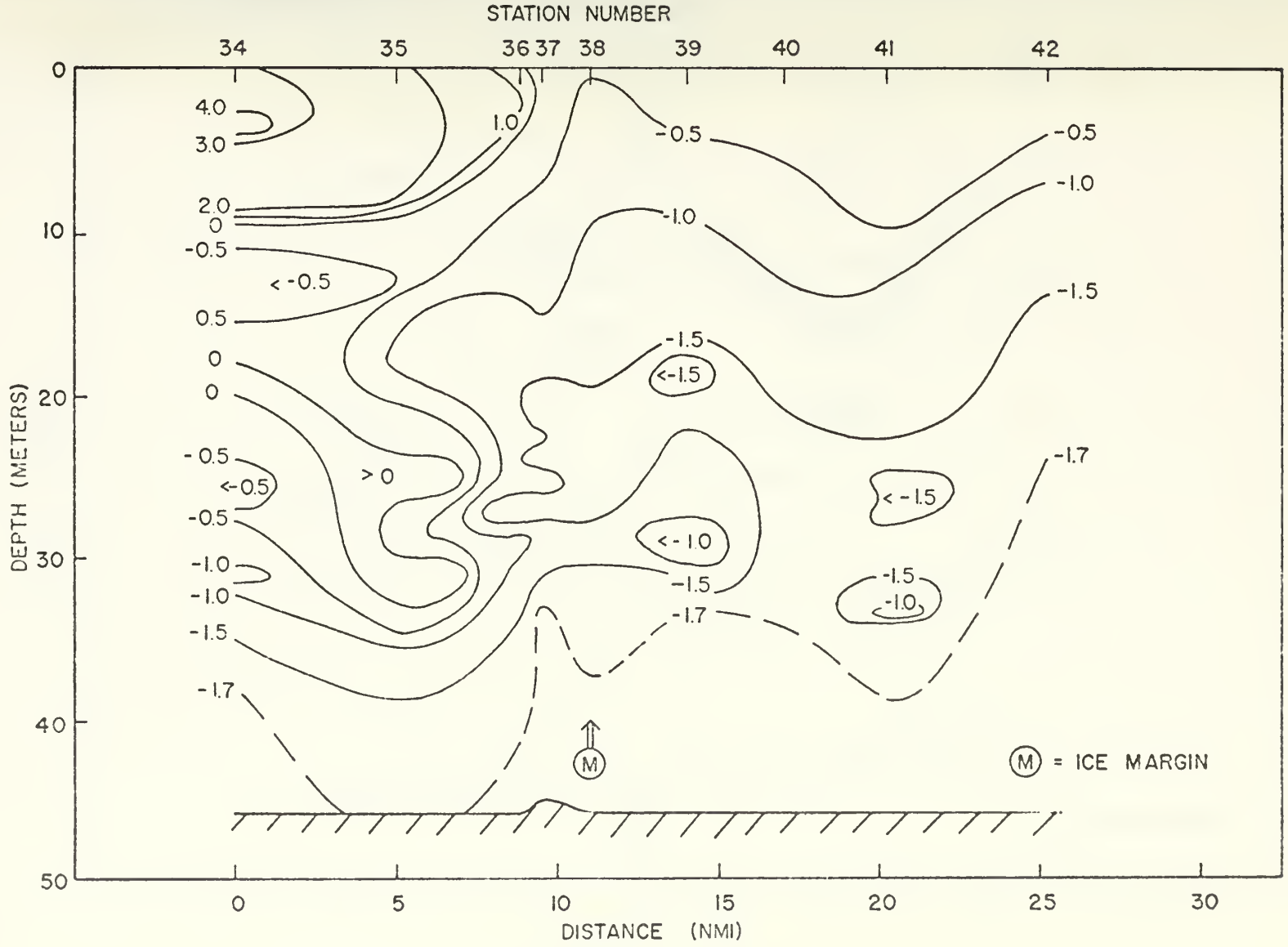

Figure 11. Temperature Cross Section, Crossing 2.

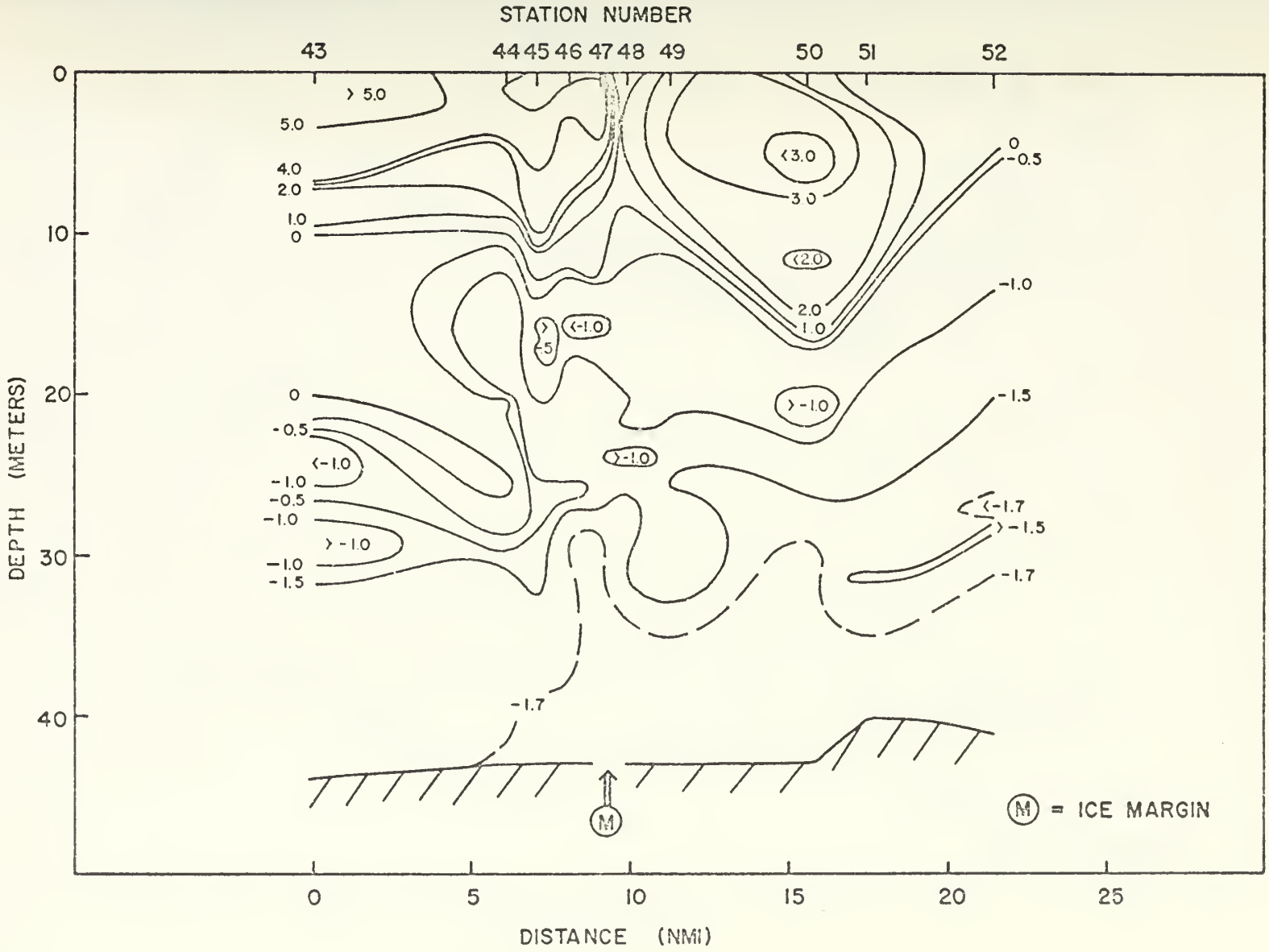

Figure 12. Temperature Cross Section, Crossing 3.

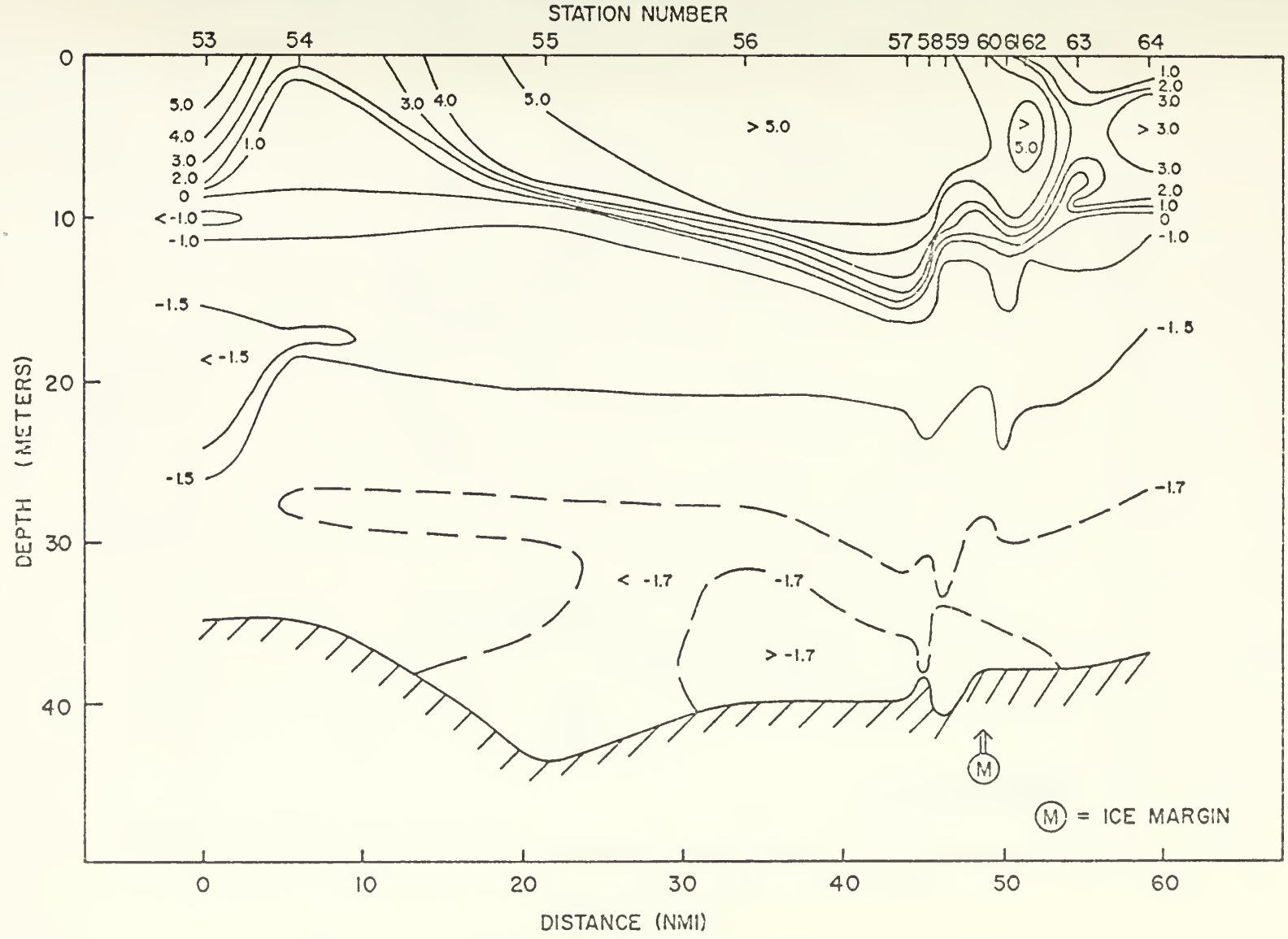

Figure 13. Temperature Cross Section, Crossing 4.

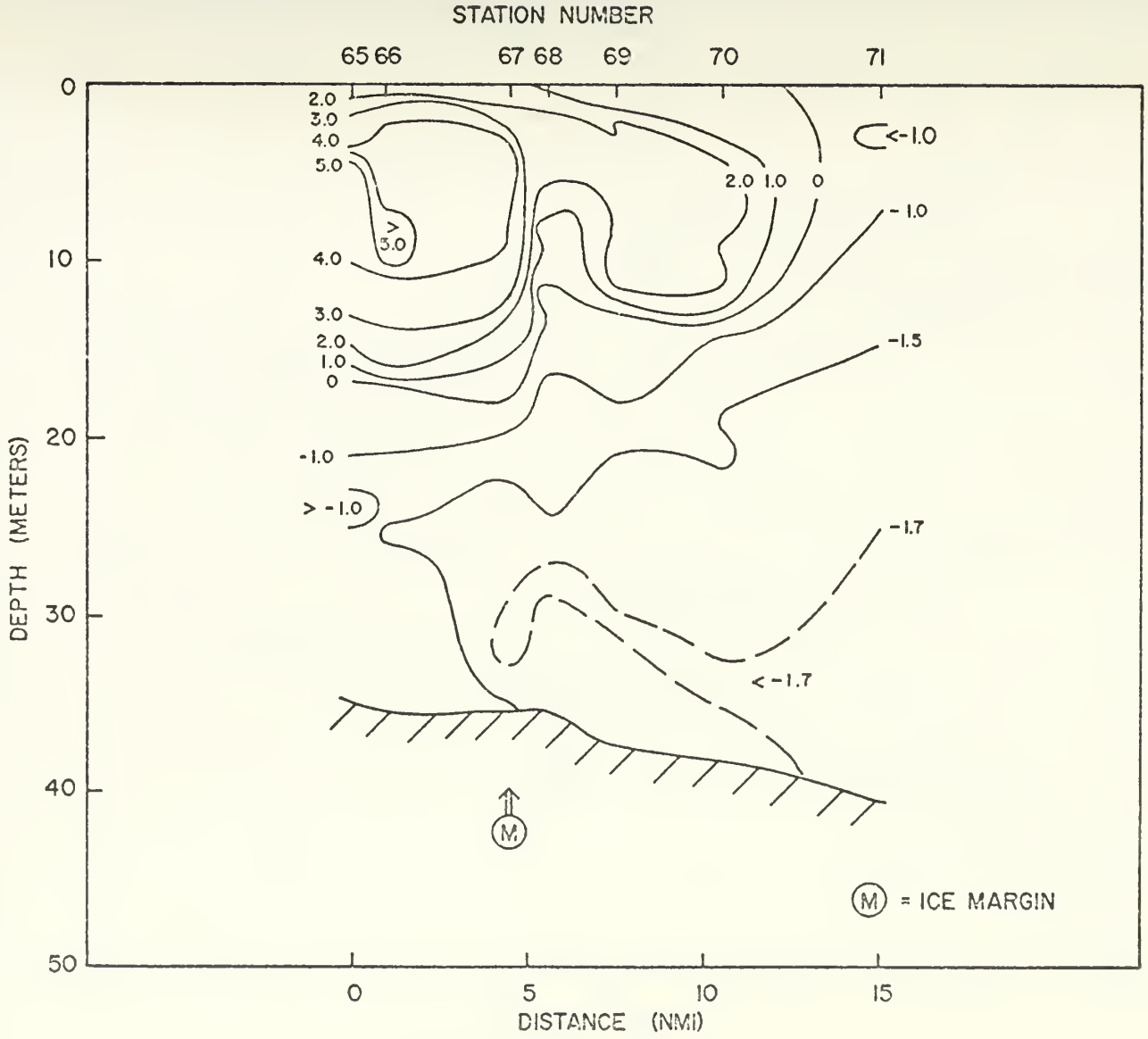

Figure 14. Temperature Cross Section, Crossing 5.

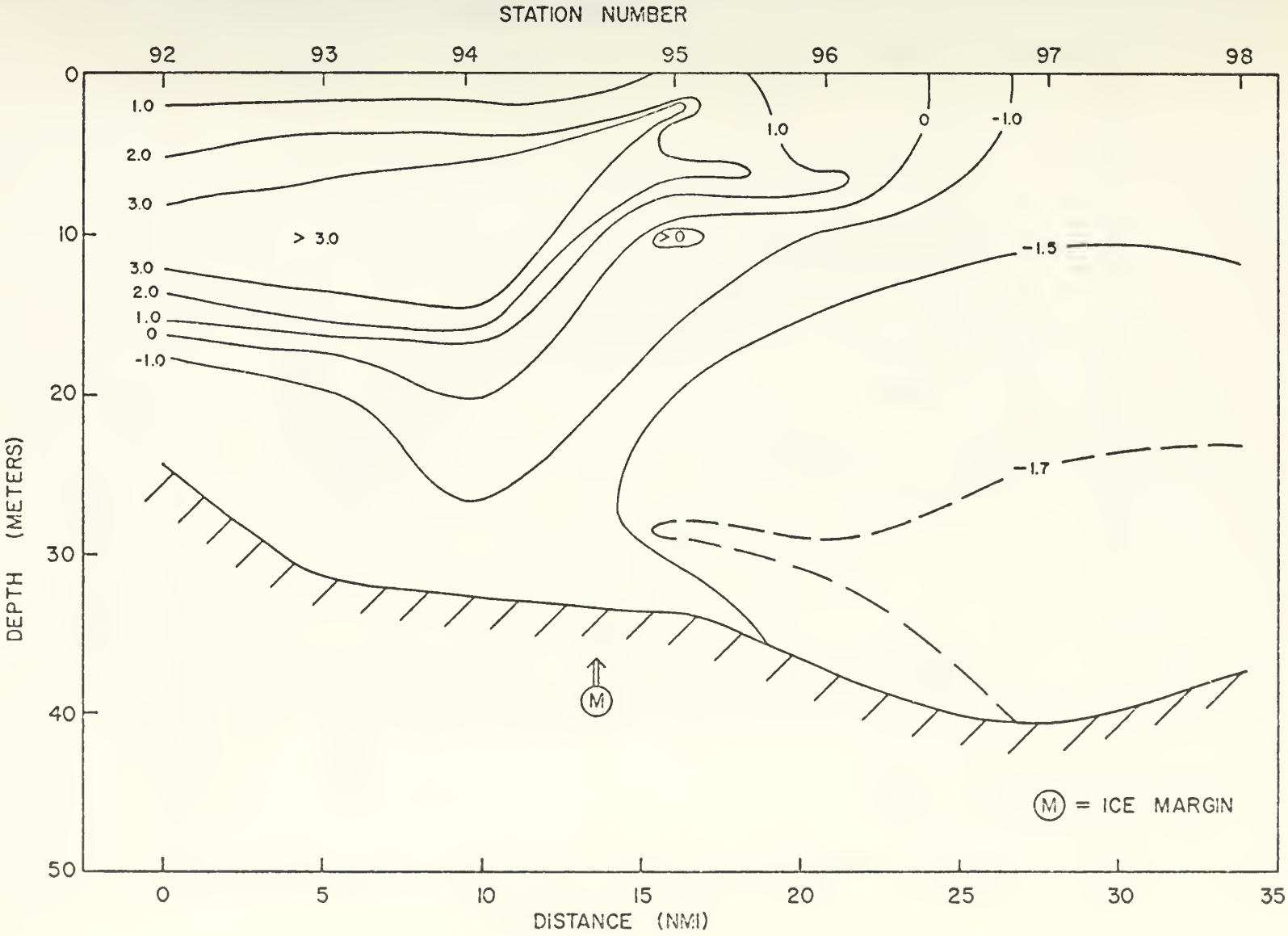

Figure 15. Temperature Cross Section, Crossing 6.

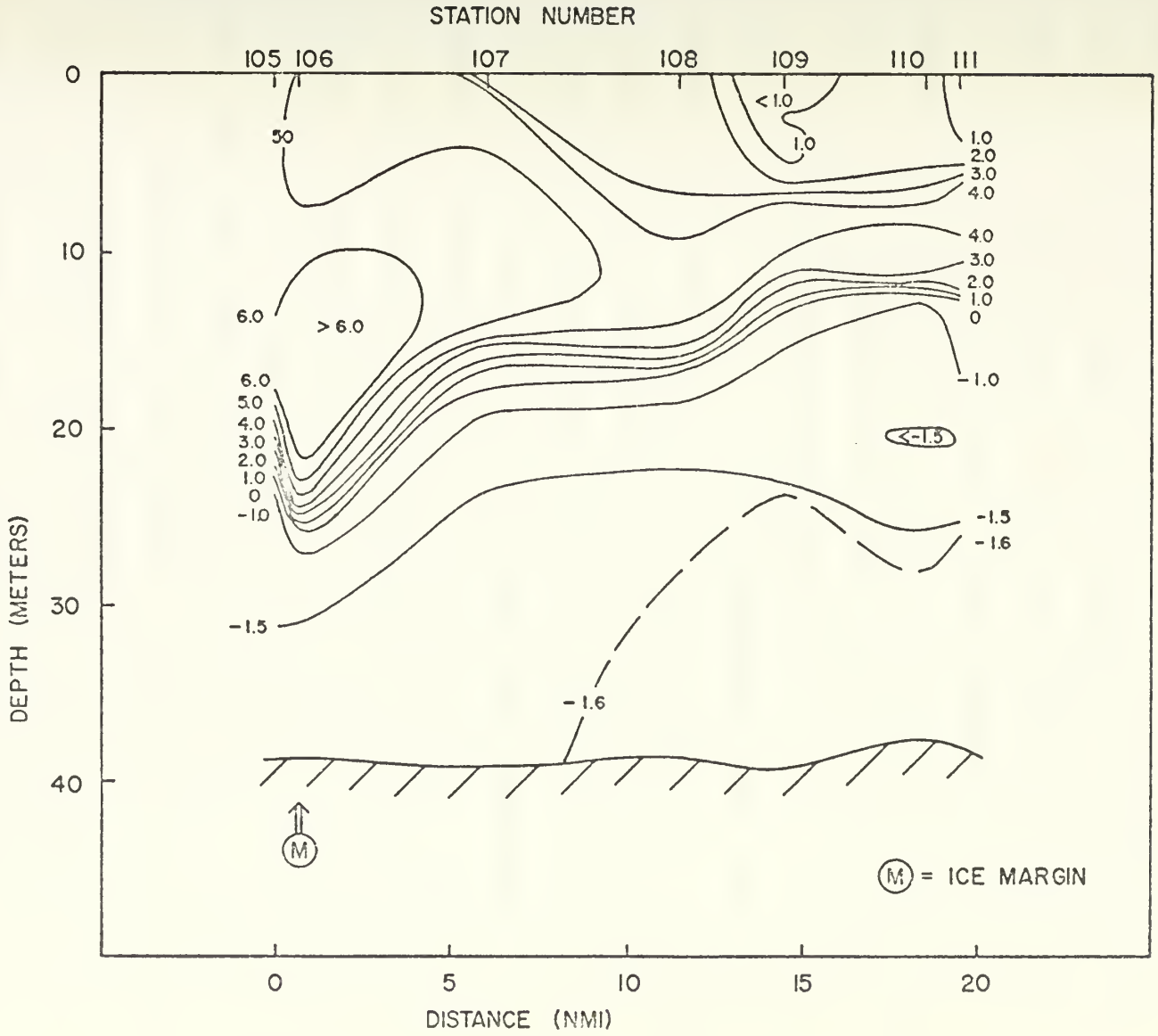

Figure 16. Temperature Cross Section, Crossing 7.

Also well correlated with the ice margin was the presence of cold bottom water which was absent to the south of the margin. This type of water appeared fairly precisely at the margin and thickened as one progressed into the ice. It had a temperature of -1.6 to -1.7°C and was usually either in the form of a wedge, as in Crossings 1, 2, 3, and 7, or that of a cold tongue at about 30 m depth as in Crossings 4, 5, and 6. This correlation of the boundary of the cold bottom water with the ice margin is indicative of the transfer of heat downward in the water column near the margin.

The dissipation of the surface heat across the margins, the melting of the ice, and the absence of the cold bottom water south of the margin all indicate large heat transfers throughout the entire water column in the vicinity of the ice margin. The extreme temperature gradients associated with the presence of structure were found predominantly near the ice margin, but not far under the ice, indicative of strong downward mixing processes in the vicinity of the margin. Farther back under the ice, however, this powerful downward mixing of near-surface water appeared to be lacking. Therefore, ice keels probably are not the cause of mixing as was suggested by Corse (1974). Instead, the mixing must be due to a dynamic process which is peculiar to the ice margin. The process must be due to something distinctive of the ice margin, most likely the rapid melting of ice. This melting process and its relationship to the formation of mesostructure will be discussed in a subsequent section.

B. DENSITY CHARACTERISTICS

The cross-sectional density distributions, plotted in sigma-t units, are shown in Figures 17 through 23. All crossings were typified by a high gradient layer in the upper 10 m, with localized pockets of low density water located at the surface which correspond to areas of melting ice. The density surfaces like the isotherms, displayed irregularity in the vicinity of the ice margin. However, the density surfaces, unlike the isotherms, displayed no inversions. The density at the surface was observed to be higher outside the margin and decreased near it. These phenomena were undoubtedly due to melting processes. The irregularity, high density gradients, and low density pockets did not appear farther back under the ice. The rapidly added melt water must have been mixed downward rather quickly in the vicinity of the margin so as to have decreased the high gradients that were present. The density cross sections display the same general characteristics as do the temperature cross sections and there is evidence of dynamic activity in all cases.

The deepest isopycnals, present well inside the ice margin, were destroyed by downward mixing of melt water near the margin. These isopycnals usually rose toward the interior of the ice field, forming a wedge-like feature. In Crossings 1, 2, 3, and 4 the wedge was pronounced. In Crossings 5 and 6 the wedge was less pronounced and did not exist in Crossing 7. This wedge was well correlated

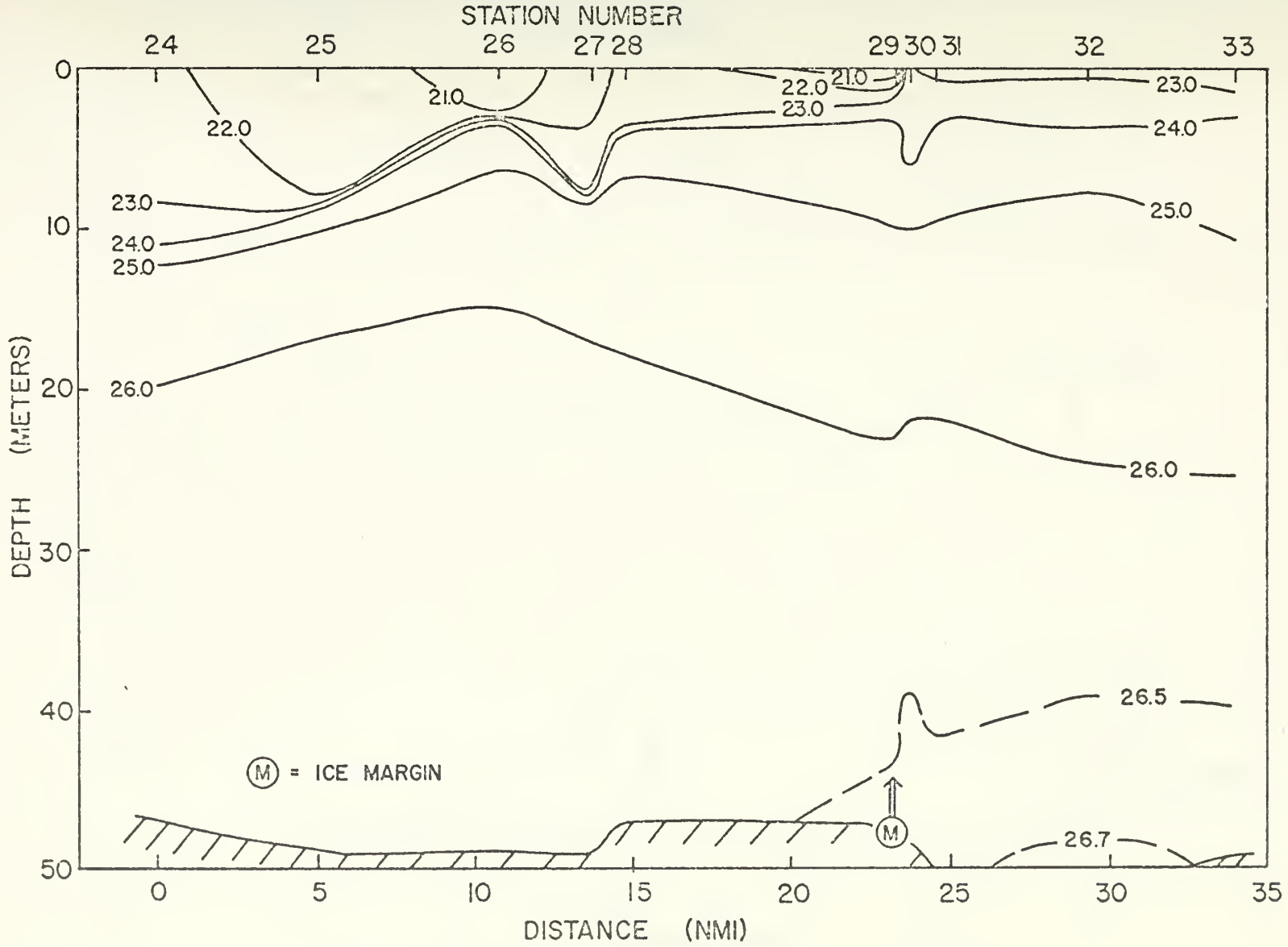

Figure 17. Sigma-t Cross Section, Crossing 1.

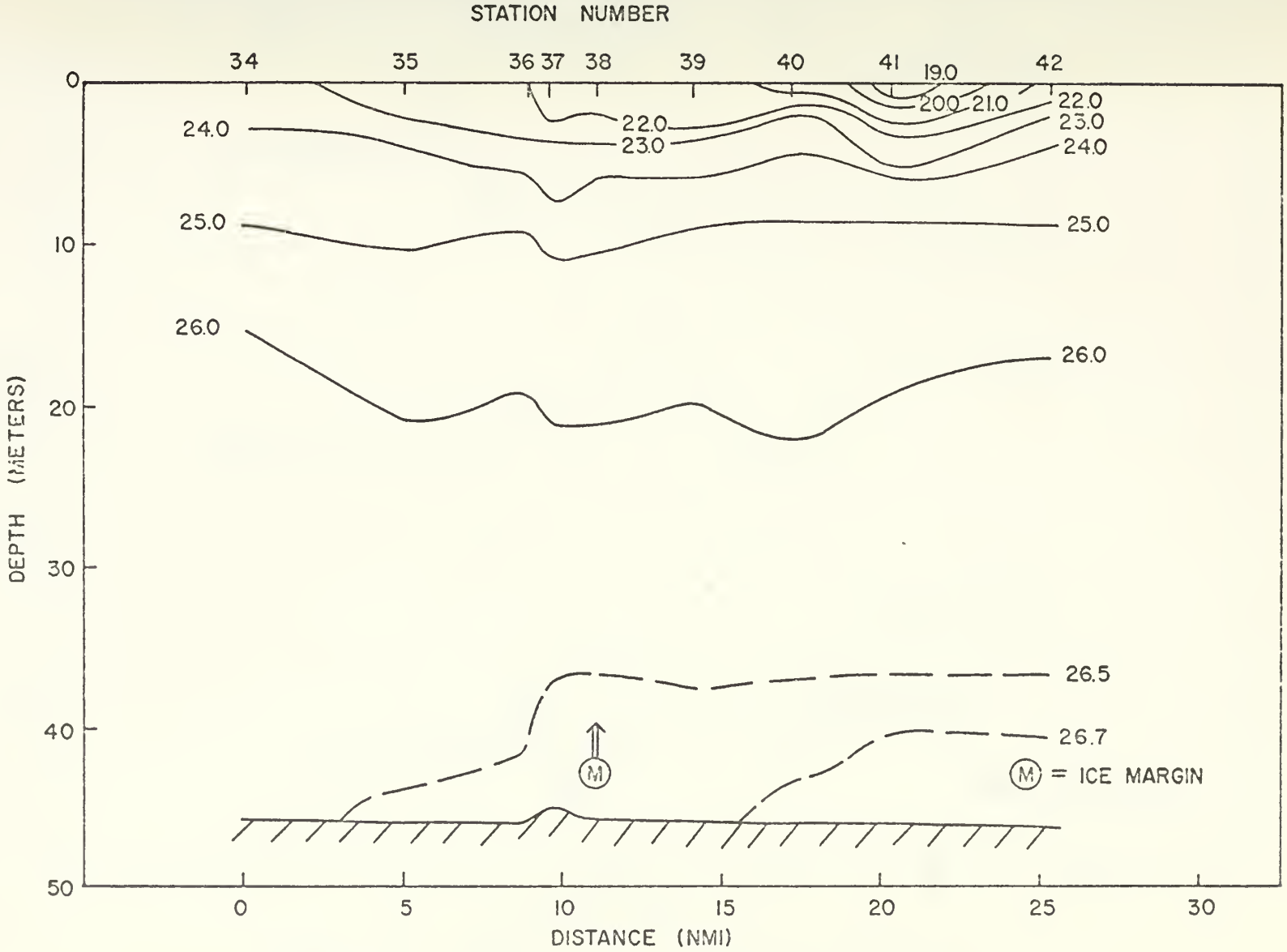

Figure 18. Sigma-t Cross Section, Crossing 2.

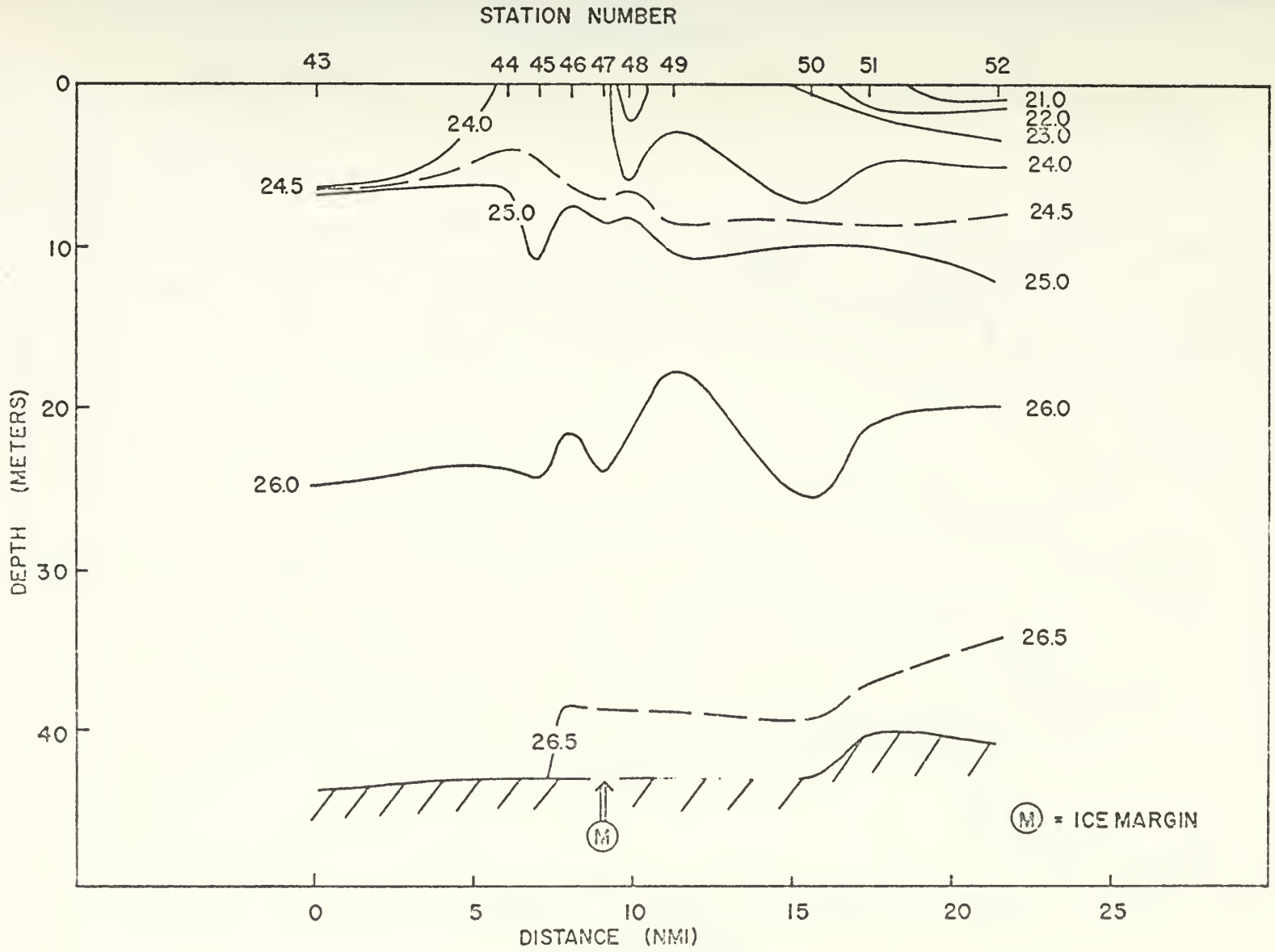

Figure 19. Sigma-t Cross Section, Crossing 3.

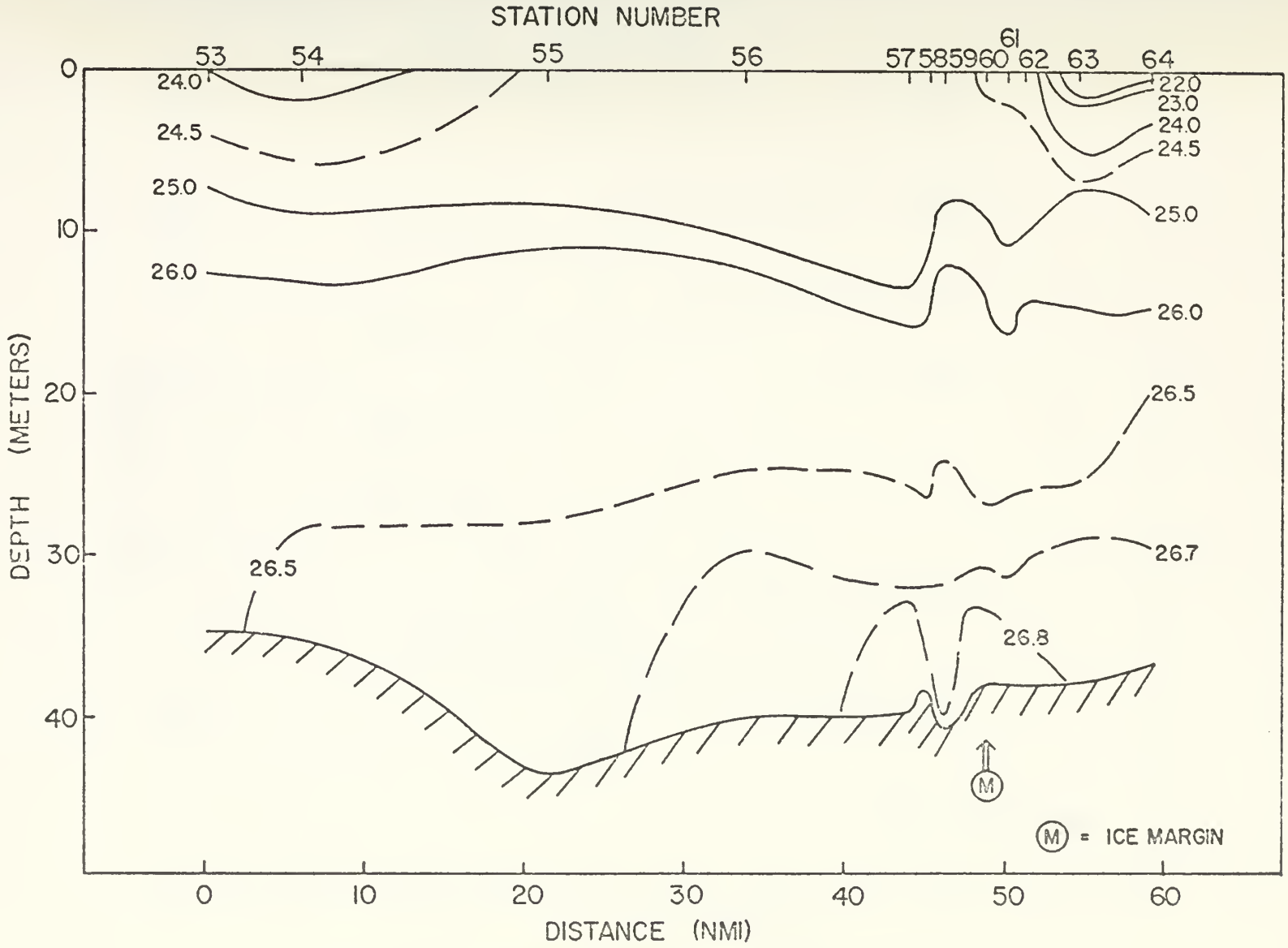

Figure 20. Sigma-t Cross Section, Crossing 4.

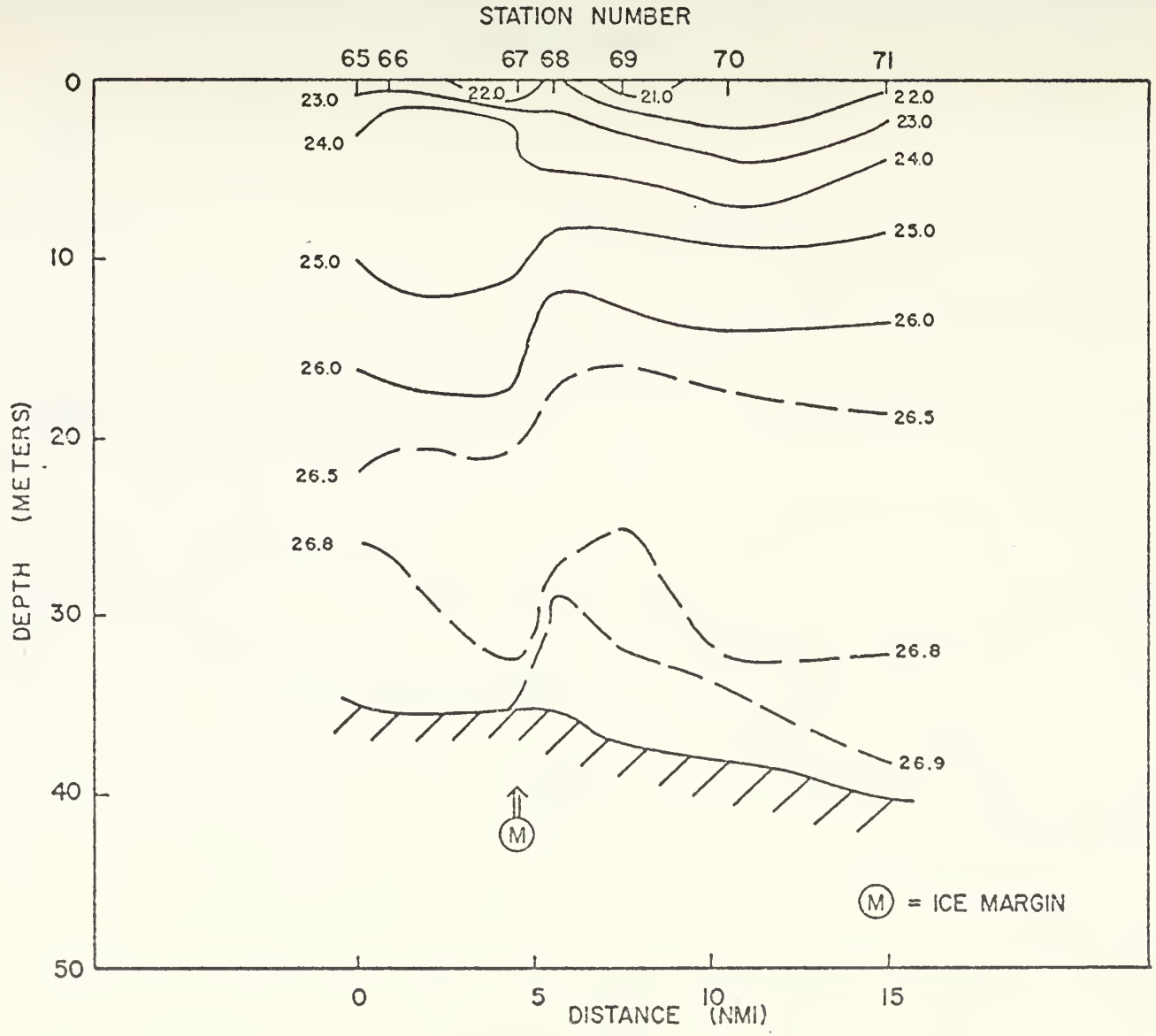

Figure 21. Sigma-t Cross Section, Crossing 5.

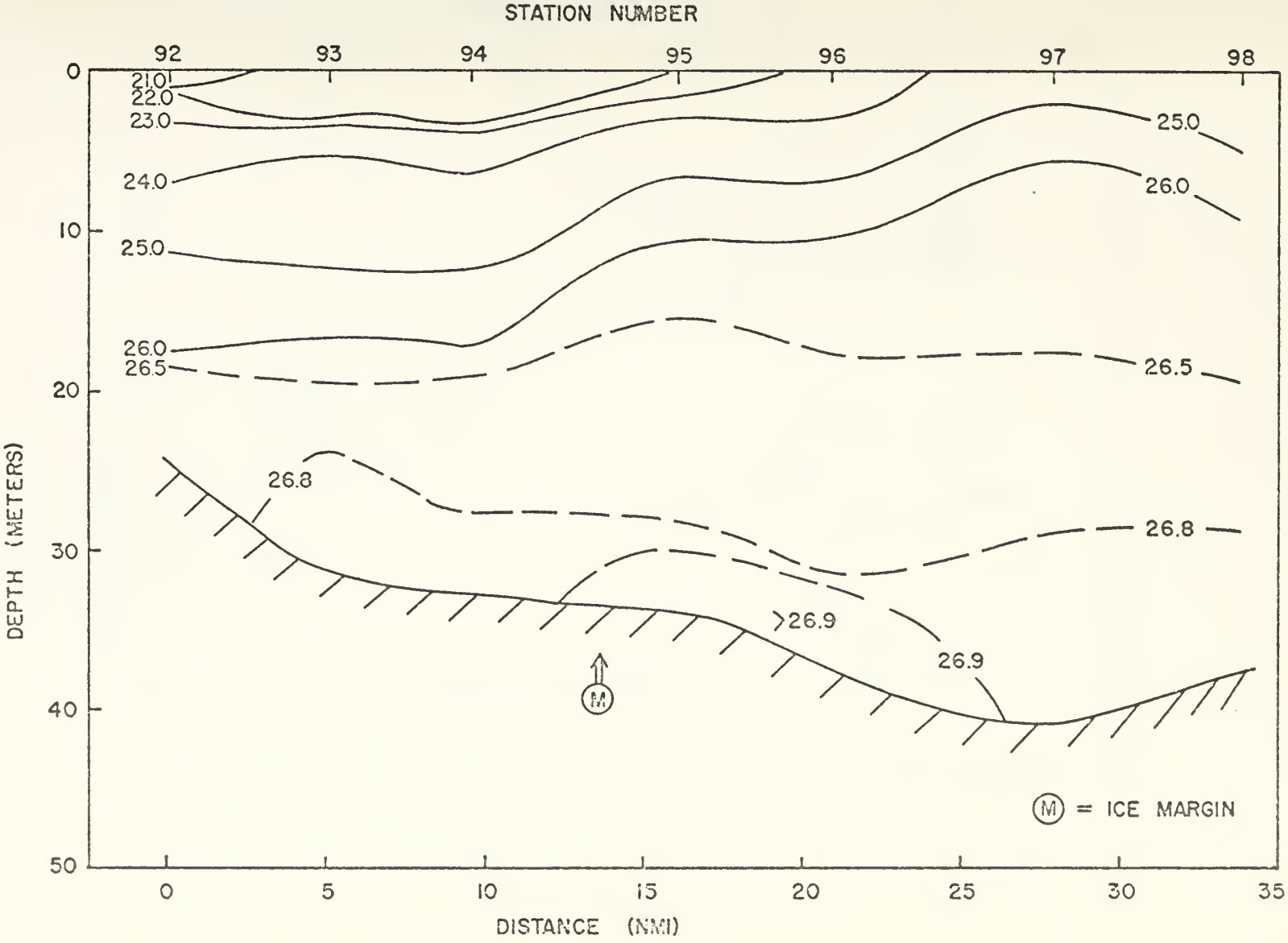

Figure 22. Sigma-t Cross Section, Crossing 6.

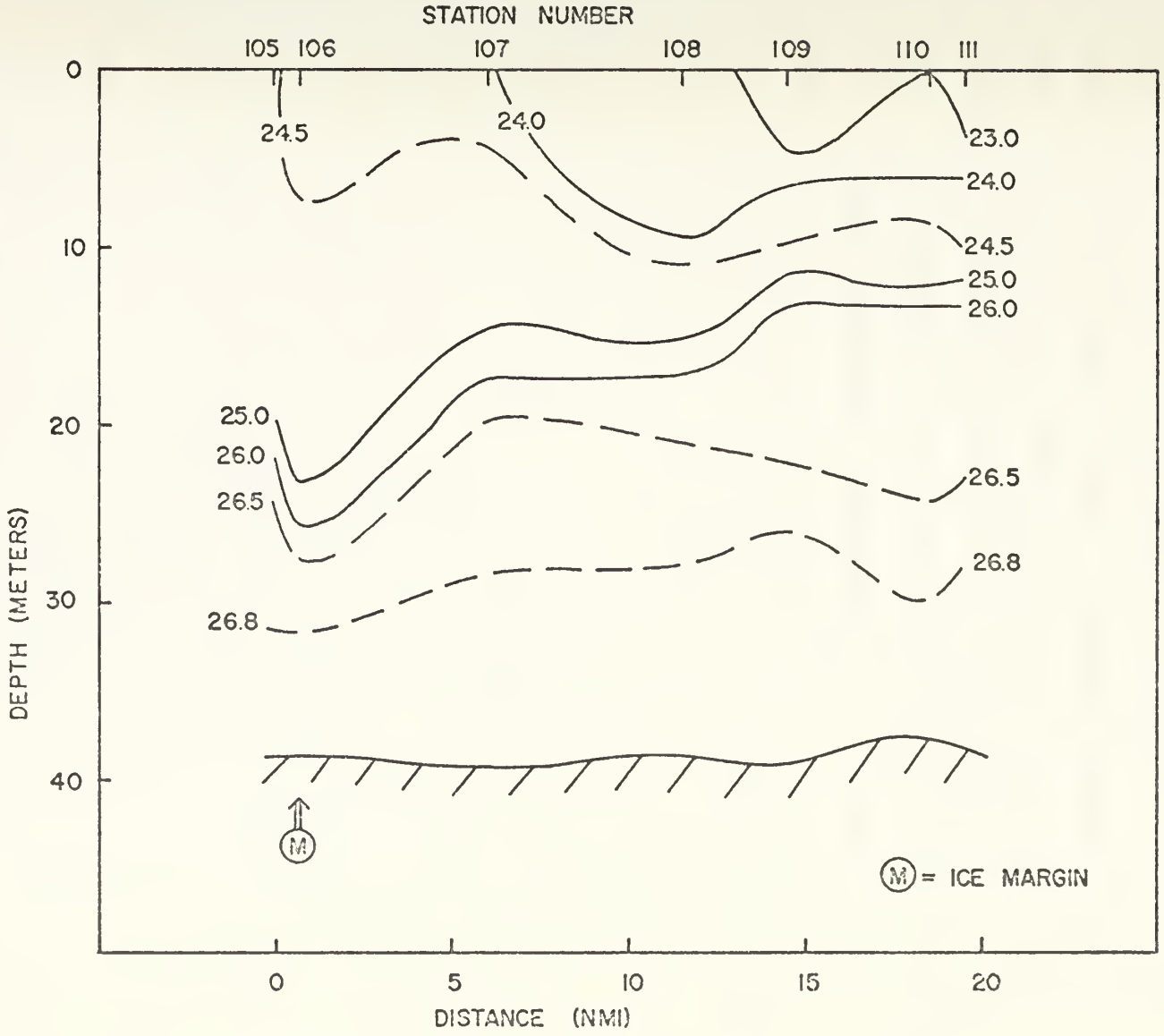

Figure 23. Sigma-t Cross Section, Crossing 7.

with the cold, bottom water found in the temperature data.

The complex tilting of the density surfaces is evidence of lateral pressures that must be maintained by dynamic processes. Thus, stronger density structures should be indicative of strong dynamic processes and more severe mesostructure. Deep mesostructure was found to be more severe for those crossings with a well-defined wedge and thus gave support to this hypothesized relationship between deep mesostructure and strong dynamic processes. This relationship was further confirmed by an investigation of the dynamic heights associated with the marginal ice zone and is discussed in a subsequent section.

Observations of the 26.0 and 26.5 sigma-t surfaces revealed that they had a pattern of variable spacing related to the ice edge. For Crossings 1, 2, 3, and 4 (Figures 17-20) these isopycnals were more widely separated outside the ice margin, thus defining a zone of very low vertical density gradient. For Crossings 5, 6, and 7 (Figures 21-23) this low density gradient zone was found well inside the ice edge, but in Crossing 5 it occurred between the 26.5 and 26.8 sigma-t surfaces. Inspection of the above figures indicates that most of the deep mesostructure is found within these zones of weak density gradient. This is perhaps an expected phenomenon as relatively little energy is required to mix anomalous water downward in the water column when the density gradient is small.

It is important to remember at this point that a temperature or density cross section suggests that there is a transport of properties from left to right. This need not be the case; flow may be oblique or nearly parallel to the ice edge. This type of flow pattern may account for small degrees of tilt to the isopycnals within the ice or for weak dynamics and weak structure to exist. It may also cause a low rate of heat transport to the ice and consequently low melting rates. Considering these factors the heat balance across the ice margin was investigated.

C. HEAT BALANCE ACROSS AN ICE MARGIN

The disappearance of the warm surface water under the ice margin and the melting which occurred led to an analysis of the heat content of the water columns associated with the ice margin crossings. Specifically, it was desired to correlate the amount of heat dissipated at the margin with the melting of an equivalent amount of ice and to test the associated idea that water flows along the section toward the ice. If it did not, it might be an explanation for weak dynamic mixing processes and weak structure.

The heat content of the water column at each station in the various crossings was calculated, using as a reference water of 33.33°/₀₀ and -1.8°C. This reference was selected since 33.33°/₀₀ is the salinity of freezing sea water at the lowest water temperature observed in the area. The resultant values were termed the "heat excess"

as defined by equation (1):

$$H = C_p \int_0^D \rho(T-T_R)\, dz \qquad (1)$$

where: H = Heat excess (cal-cm^{-2})

C_p = Specific heat (cal-gm^{-1} °C^{-1})

ρ = Density (gm-cm^{-3})

T = Temperature (°C) at depth z cm

T_R = Reference temperature (°C)

D = Depth of the water column (cm)

dz = Depth increment (cm)

In order to examine the melting phenomenon in terms of the fresh water introduced from melting ice an "ice melt content" was also defined. It was defined as that weight of ice, with an initial salinity of 6.0°/$_{oo}$ and a density of 0.94 gm cm^{-3}, that must be transformed into melt water to produce the salinity structure present in the given column of water, referenced again to a water column having an initial salinity of 33.33°/$_{oo}$. The ice melt content is defined by equation (2):

$$I = \int_0^D \rho\left(\frac{S_R - S}{S_R - S_I}\right) dz \qquad (2)$$

where: I = Ice melt content (gm-cm^{-2})

S_R = Reference salinity (ppt)

S = Salinity (ppt) at depth z cm

S_I = Salinity of ice (ppt)

Values of 0.956 cal gm^{-1} $°C^{-1}$ for C_p and 100 cm for dz were selected and the values for the remaining variables (T, D, ρ, and S) were obtained from the individual station data. Using these values the total integrated heat excess and ice melt content from the surface to the bottom were computed. The values from the surface to 35 m were selected for comparison purposes for the analysis. One may make nearly as good an argument for integrating to the bottom. However, the likelihood of incorporating an anomalous contribution from a variable depth limit led to the choice of a fixed limit. The results of these computations for all crossings are displayed in Table I.

Ideally, with a flow of water directly across the ice margin, the heat excess and ice melt content data should present an inverse relationship. The heat excess should decrease and remain low after passing the margin as the ice melt increases, which in turn should remain high due to the melting process. Considering the heat excess and ice melt content data, many irregularities were present in each of the crossings. However, all crossings did display a general heat decrease and an increase in ice melt content close to the ice margin, except for Crossing 6 which displayed a decrease in ice melt content and heat excess. Crossing 2 is presented as an example (Figure 24). It was close to the average of all the crossings, excluding Crossing 6, even to the extent of being less irregular than most. The data from the seven crossings revealed a decrease

Crossing Stations	Ice Melt Content (gm cm^{-2}) Heat Excess ($cal\ cm^{-2}$)										* = Ice Margin	
1	304	309	248	301	252	256	254	241	243	282		
					*							
24 - 33	15920	12140	7376	8641	7148	3220	2722	3247	1814	1376		
2	209	256	261	296	281	282	265	--	239			
					*							
34 - 42	8291	7786	3473	2733	2030	2212	2008		1708			
3	211	205	228	205	220	260	226	243	269	277		
					*							
43 - 52	9025	7439	8739	7034	6874	4238	6390	8371	5946	2589		
4	165	186	139	140	159	152	133	150	165	150	210	195
								*				
53 - 64	6450	3150	7567	9461	11160	10740	8796	7912	8938	8379	4311	4984
5			167	166	201	180	--	231	211			
					*							
65 - 71			10280	11210	8969	5380		5423	1342			
6		250	230	235	156	144	85	146				
					*							
92 - 98		7000	8400	9400	4714	2966	971	1112				
7				180	223	158	245	211	205	218		
					*							
105 - 111				16770	18890	12520	9654	6201	6351	6483		

Table I. Heat Excess and Ice Excess for Crossings 1 to 7.

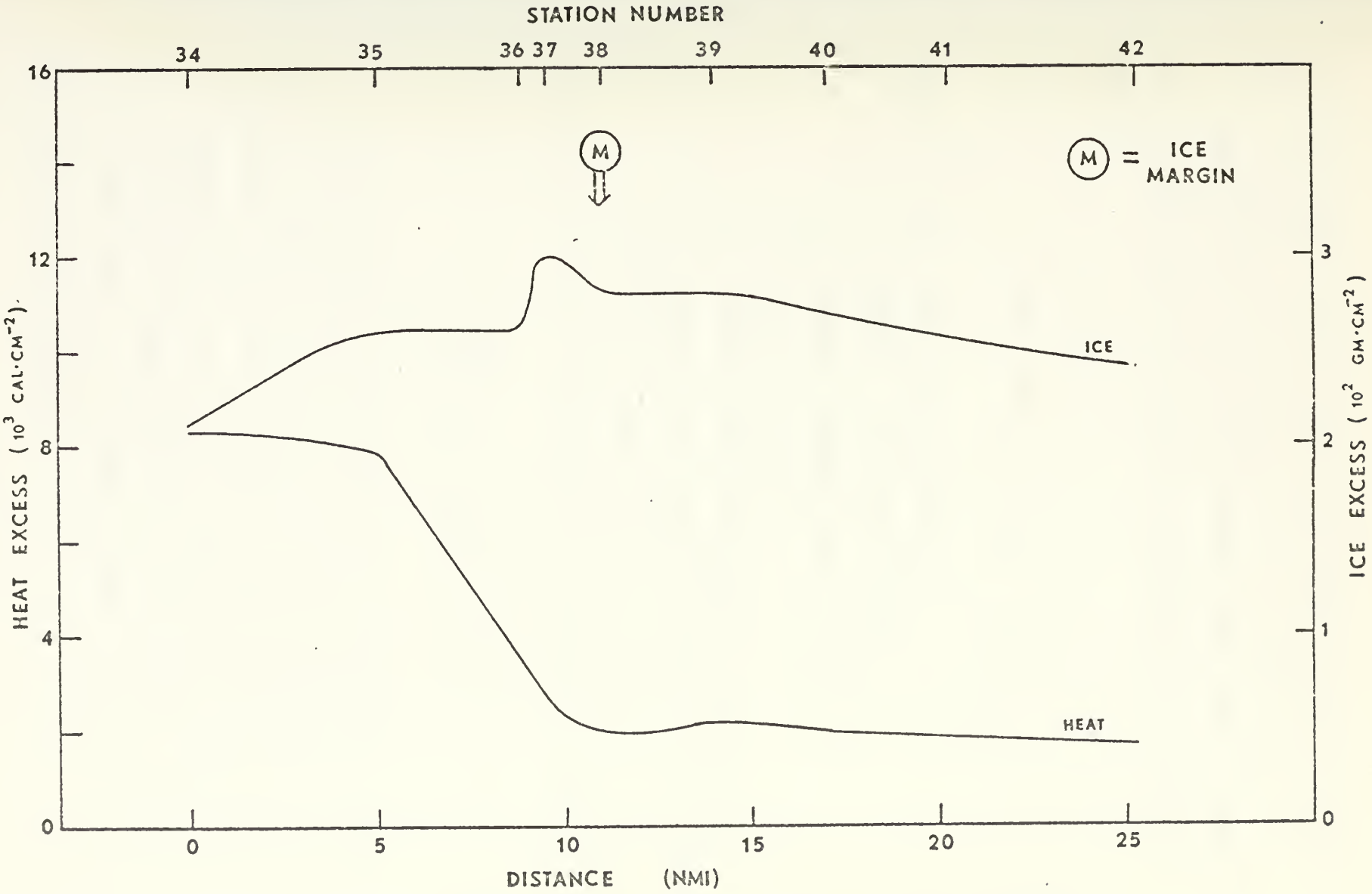

Figure 24. Heat Excess and Ice Melt Content for Crossing 2.

in excess heat ranging from 4900-10300 cal cm^{-2} across the ice margin. The average change was 6600 cal cm^{-2}.

Equation (3a) describes the heat (ΔH) that is required to warm and melt ice of initial temperature T_o and thickness h

$$\Delta H = [(T_g - T_o)\ C_p + \lambda_I]h\rho \qquad (3a)$$

where: ΔH = Heat change (cam cm^{-2})

T_o = Initial temperature (°C)

T_g = Melting temperature (-.053S) (°C)

S = Salinity (ppt)

C_p = Specific heat of fresh ice (cal $gm^{-1}°C^{-1}$)

λ_I = Latent heat of fusion of sea ice (cal gm^{-1})

h = Ice thickness (cm)

Solving for the ice thickness, h, we arrive at equation (3b):

$$h = \frac{\Delta H}{\rho}\ [(T_g - T_o)\ C_p + \lambda_I]^{-1}. \qquad (3b)$$

An ice cover of salinity 6.0°/$_{oo}$, initially at -2°C, and with a density of 0.94 gm cm^{-3} was selected as representative of the area of study. This selection resulted in values of 0.5 cal $gm^{-1}\ °C^{-1}$ for C_p and 67 cal gm^{-1} for λ_I. Using the average change of heat content, 6600 cal cm^{-2}, across the margin and the above values, an ice thickness of 1.0 m would be melted.

The ice melt content, with one exception, displayed an increase across the margins of 30-73 gm cm^{-2} with an average value of 54 gm cm^{-2}. The exception was Crossing 6 which resulted in a negative value. The average value of 54 gm cm^{-2} when equated to a thickness of reference ice by equation (4) resulted in an equivalent ice thickness melted of 0.6 m:

$$h = \Delta I \rho^{-1} \tag{4}$$

where: h = Thickness of ice melted (cm)

ΔI = Change in ice excess ($gm\text{-}cm^{-2}$)

ρ = Density of ice ($gm\text{-}cm^{-3}$).

The values of the thickness of ice melted computed from the heat excess and ice melt content agree favorably with the ice thickness of about 0.8 m predicted for the region of study by Wittman et al. (1963). This lends support to the assumptions that the dissipation of the heat across the ice margin can be accounted for by the melting of the ice cover and that the flow under the ice margin is generally northward (left to right in the sections).

The overall changes in heat excess and ice melt content across the margin were not apparently related to the severity of structure present (Table III). However, the rates at which they changed near the margin were possibly related to the severity of shallow mesostructure. Crossings 1 and 2 had the least rapid heat and melt water changes in the vicinity of the margin and also displayed the least

severe shallow structure. Crossings 3, 4, and 5 had significantly more rapid heat exchanges at the margin and also had the more severe shallow structure. These factors suggest a correlation between the rate of heat exchange and the severity of shallow structure.

In most cases the major portion of the heat exchange occurred at the ice margin; however, in Crossings 1 and 2 it occurred outside the ice margin. This can be explained by a flow away from the ice subsequent to a period of melting or by a retreat of the ice front that was more rapid than the northward flow of water.

In Crossings 1, 3, 4, 5, and 7 there was an irregular increase of ice melt content toward the north which is what one might expect if the melt water near the margin were carried under the ice by the current. Crossings 2 and 6 displayed a gradual decrease of ice melt content as one progressed farther under the ice. Possible explanations for this difference are that the axis of flow of the northward current was not directly across the margin or an irregularity of flow occurred. Thus, it appears that the flow at the margins is not as simple as was assumed, although it is generally northward.

D. DYNAMIC HEIGHTS AND LOCAL CURRENTS

The degree of disturbance in the density surface (Figures 17-23) and the presence of many factors which pointed to the existence of highly dynamic processes acting

in the immediate vicinity of the ice edge gave rise to an interest in the dynamic heights associated with melting at the marginal ice zone. Neshyba's model (1974) of the prograding ice cover during the freeze-up of the Bering Sea predicted the inverse phenomenon, a dynamic low under the ice margin. His model described the freezing process which rejected brine and mixed it downward through the entire water column resulting in higher density, a dynamic low, and a horizontal pressure gradient toward the ice under the freezing zone. Neshyba concluded that freezing rates were slow enough such that the pressure gradient must be in geostrophic balance and must therefore correspond to a geostrophic flow to the east under the freezing zone. His assumption that the oceanic system was otherwise static probably led to unrealistically high values of salinity and correspondingly high negative values of dynamic height. An extension of Neshyba's work to the melting season would suggest that the converse situation, a dynamic high, might be found under a melting ice zone and, with melting much more rapid than freezing, that the change in geopotential should be much greater.

Dynamic heights for all crossings were computed utilizing the HYDRO program (W. R. Church Computer Center, NPS) and the results appear in Table II. Figure 25 presents a vertical cross-section of dynamic heights for Crossing 2 which was selected to illustrate significant features. All crossings in general displayed local irregularities and

Crossing Stations	Dynamic Height (dyn cm) (* - Ice Margin)											
1 (24 - 33)	12.3	12.8	10.5	11.7	10.6*	10.8	10.4	10.5	10.3	12.5		
2 (34 - 42)	9.2	10.7	10.6	11.2	12.0*	11.3	11.1	--	10.8			
3 (43 - 52)	9.9	9.7	10.2	9.7	10.0*	10.5	10.0	10.8	11.5	11.5		
4 (53 - 64)	8.0	8.4	7.6	7.7	8.2	8.0	7.5	7.9*	8.2	8.5	9.0	9.2
5 (65 - 71)			8.2	9.3	9.4*	8.8	8.9	8.5	8.4			
6 (92 - 98)		10.1	9.7	9.8	8.6*	8.4	6.1	7.5				
7 (105-111)				9.0	10.0*	8.2	9.7	8.8	8.7	9.0		

Crossings 1, 2, 3, and 4 referenced to 40m; 5, 6, and 7 referenced to 35 m.

Table II. Dynamic Heights for Crossings 1 to 7.

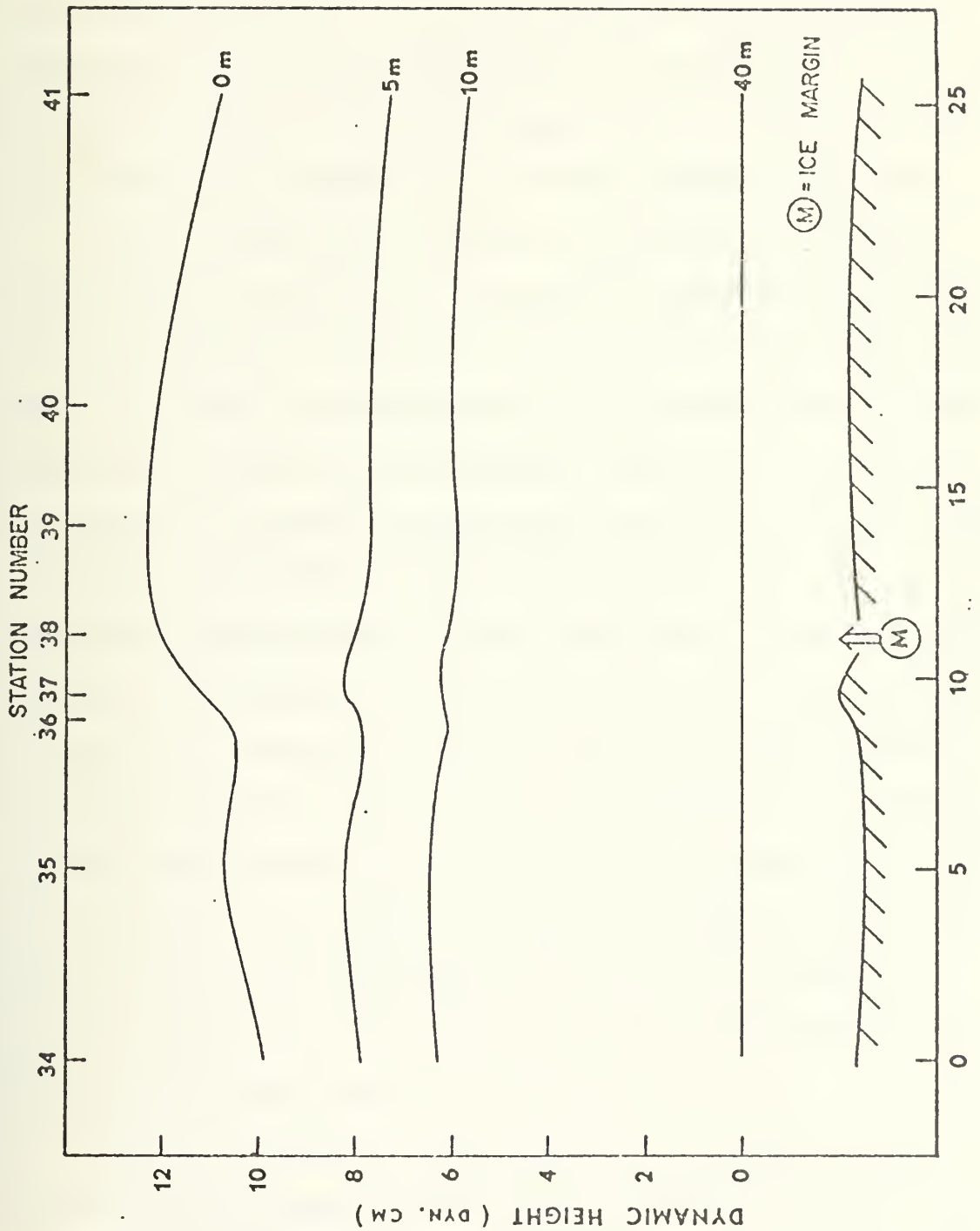

Figure 25. Dynamic Heights for Crossing 2.

all, with the exception of Crossing 6, displayed a hill (or half of a hill as in Crossings 1, 3, and 4) situated near the ice margin. Evidence of this dynamic hill was observed to a depth of about 10 m in Crossings 1, 2, 3, and 4 and to about 15 m in Crossings 5 and 7. Thus the hill was generally noticeable in the near surface zone only.

These results were somewhat as predicted. However, the hill was found to be a localized phenomenon extending over horizontal distances of up to 30 km across the margin and its effects were observed to only about 10 m of depth. This was different from Neshyba's freezing model which resulted in a general depression associated with the entire freezing zone which extended 100 km back under the ice, and whose effects were notable throughout the entire water column. The heights of these hills were of the order of 2 dyn cm as compared to depressions of 2.7 dyn cm calculated by Neshyba. The hills due to melting were expected to have been several times as large as the depressions due to freezing, but were not. This was probably because the water at the ice margin was not static as in Neshyba's model. It will be seen, however, that the magnitude of this hill is not the critical factor.

The author's data revealed that the height of the hill under the ice apparently was not correlated with the severity of the mesostructure. However, the magnitude of the horizontal gradient of the dynamic height at the margin did appear to be related directly to the severity and presence

of deep mesostructure. Table III shows that Crossings 1, 2, 3, and 7 had the highest dynamic height gradients and also the most severe deep structure, whereas Crossings 4 and 5 had relatively small gradients and either lacked or had very little deep structure.

The gradient observed in the dynamic heights must result in a lateral pressure gradient. This gradient is probably of recent origin due to the rapid retreat of the ice margin; thus geostrophic balance is probably not achieved and the pressure gradient is most likely balanced against inertial acceleration or internal friction. In either case the pressure gradient leads to a velocity shear in the vertical plane normal to the ice margin. Because the pressure gradients on the two opposing sides of the dynamic hill are oppositely directed, there will be a diminution of flow near the surface on the seaward side of the dynamic hill and an acceleration of flow on the other. Continuity of flow then would demand that the shear at the surface be compensated by a reverse shear at deeper depths under the dynamic high. It is believed that this downward directed flow may be the agency which caused the mixing at depth which was observed near the ice margin.

Both of the possible opposing forces of friction and inertia were found to be of the same order of magnitude, depending upon one's choice of viscosity and characteristic velocity, but viscosity is likely to exert the largest effect. Therefore, to explore the magnitudes of the

Crossing	Structure Intensity (0→5) (None→Severe)		Nose Feature Well Defined	Decrease in Heat across the Ice Margin (10^3 cal cm^{-2})	Increase in Ice Melt Content across the Ice Margin (10^3 gm cm^{-2})	Dynamic Gradient at the Margin (dyn m km^{-1})
	Shallow	Deep				
1	1	5	No	5.7	30	.0022
2	1	5	No	6.6	73	.0039
3	5	5	No	6.4	66	.0025
4	2	1	Yes	6.2	50	.0010
5	3	1	Yes	4.9	64	.0016
6	3	0	Yes	5.9	-104	-.0108
7	2	2	Yes	10.3	38	.0027

Table III. Comparison of Crossings.

effects, approximate calculations were made based on the assumption that the lateral pressure gradient was balanced by the frictional shear of eddy viscosity. A model was developed assuming a current, u, outside the ice, flowing in the plane of the pressure gradient and uniform in velocity throughout the upper warm layer.

The step-like profile of Figure 26 (solid line) was designed for the current velocity structure hypothesized outside the ice margin based on observed currents from other investigations. Equation (5) was used to describe the balance of frictional shear with the horizontal pressure gradient:

$$\frac{A}{\rho} \frac{\partial^2 u}{\partial z^2} = \frac{\Delta D}{\Delta L} \qquad (5)$$

A = Coefficient of eddy voscosity ($gm\text{-}cm^{-1}\ sec^{-1}$)

ρ = Density ($gm\text{-}cm^{-3}$)

u = Current speed ($cm\text{-}sec^{-1}$)

z = Depth (cm)

$\frac{\Delta D}{\Delta L}$ = Horizontal gradient of dynamic height ($dyn\ m\text{-}km^{-1}$).

Equation (5) was solved for u with the conditions that the dynamic effect was limited to 10 m and that z = 10 m, $\frac{\partial u}{\partial z} = 0$ and $u = 15\ cm\ sec^{-1}$. Specification of this velocity was not necessary to the solution, but it did influence to some extent the choice of A. $\frac{\partial^2 u}{\partial z^2}$ was assumed to be constant which required that ρ and A also be constants.

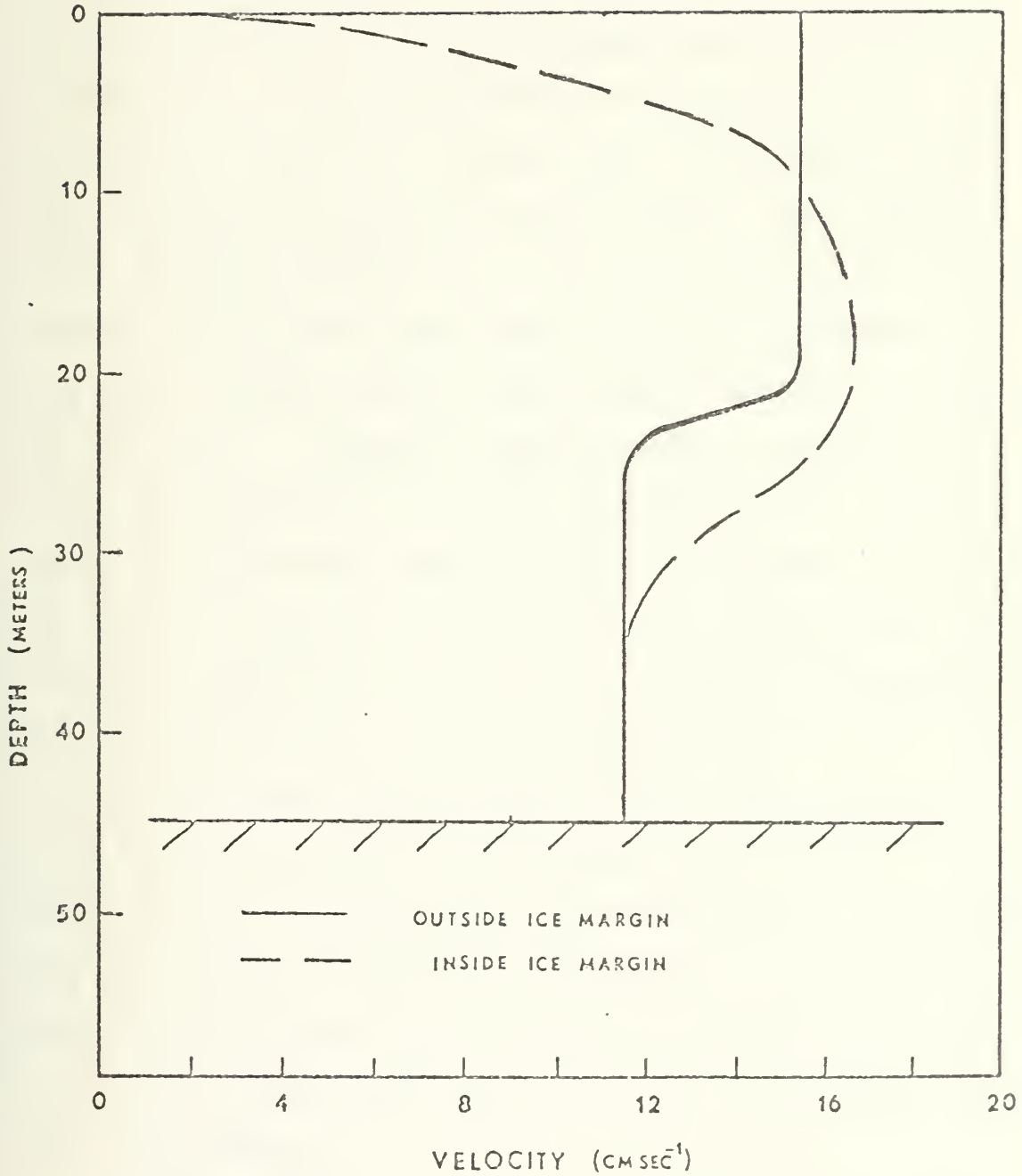

Figure 26. Effect of the Dynamic Hill on the Current Profile.

The values of the horizontal gradient of dynamic height, which were observed for the crossings, ranged between 0.0010 and 0.0039 dyn m km^{-1} with an average of 0.0026 dyn m km^{-1} for all crossings except Crossing 6 (Table III). Values for density and depth were selected as 1.02 gm cm^{-3} and 10 m, respectively. Selecting a value for the coefficient of eddy viscosity (A) was more difficult. Eddy viscosity coefficients have an extreme range of values which vary with the scale and rate of the phenomenon in question. Neuman (1966) shows values of from 1 to 3000 gm cm^{-1} sec^{-1}. Campbell (1965), however, arrived at a value of 55 gm cm^{-1} sec^{-1} for a numerical model of the ice packs of the Arctic Ocean, in which a relative velocity of 13 cm sec^{-1} existed between an ice floe and the sea water. Figure 27 shows how a variation in A affects the magnitude of the total velocity diminution experienced at the surface due to the shear forces opposed to the flow. Varying A from 50 to 500 gm cm^{-1} sec^{-1} reduces the current from 23.5 to 2.35 cm sec^{-1} which is of the proper order of magnitude for the currents assumed for the region. An intermediate value of 100 gm cm^{-1} sec^{-1} resulted in a decrease of the velocity at the surface of 13 cm sec^{-1}, a fortuitous agreement with Campbell.

The application of this velocity shear in the upper 10 m of the water column and the enforcement of continuity of flow upon the initial current profile of Figure 26 resulted in the second profile (dashed line) of Figure 26, the

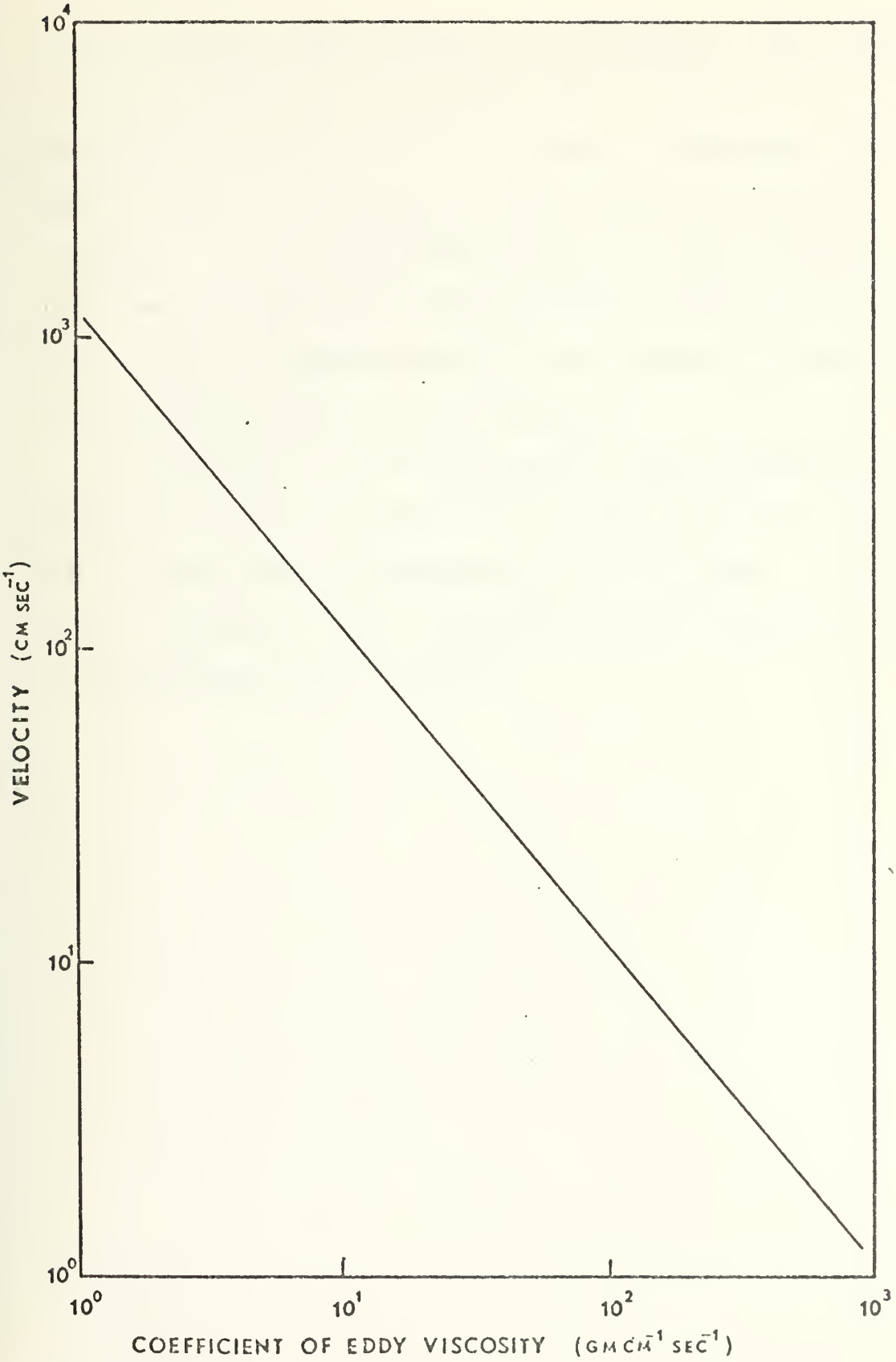

Figure 27. Effect of Eddy Viscosity on Current Velocity Diminution.

profile for the flow beneath the ice margin. This profile displays a descent of the core of the current as it encounters the margin and its effects. The compensating flow at depth is pictorial; it did not seem feasible to calculate it in a more meaningful way. This restriction to the flow, the resultant downward motion, and the acceleration of flow at greater depths could provide a mechanism for the mixing process which occurred.

It is evident that where dynamic height gradients are large, the vertical shear must be large and require greater and probably deeper compensating flows at depth. As previously discussed, these regions will most likely be areas of significant deep structure.

IV. CONCLUSIONS

A. SUMMARY OF RESULTS

The distribution of temperature, density, heat, and dynamic heights confirmed that the phenomenon of temperature mesostructure near Arctic ice margins was related to the presence of an ice margin and the associated melting processes. Mesostructure was characterized by large temperature gradients occurring simultaneously with low density gradients. It was present in a relatively broad zone, 18 to 65 km wide, across the margins. It varied considerably over short distances, with individual elements generally being traceable for only a few kilometers.

The assumption of a generally northward flow for the area of study was supported by the heat excess and ice melt content calculations. A decrease in heat content and a corresponding increase in the ice melt content of the water column was observed as one crossed the ice margin. These changes agreed reasonably well enough with the heat required and the melt water that would have been formed by the melting of the existing ice cover to support the assumption of a generally northward flow. The flow, however, displayed the possibility of not always flowing directly across the margins. Crossings 2 and 6 displayed both a heat and an ice melt content decrease as one progressed farther under the ice. This could have

indicated a flow approaching the margin obliquely and thus carrying some of the melt water away. The many irregularities also present in both the heat and ice melt results suggest the presence of complex flows near the margins.

Large heat exchanges and downward mixing throughout the entire water column were evident near the ice margins. The warm surface flow was cooled at the surface by melting to form the nose feature. The cold, dense bottom water, not present south of the margin, was dissipated by downward mixing in the water column creating a high density wedge-like feature. The broad zones of low vertical density gradient resulting from this mixing were found only near the margin and not far under the ice. Thus, the creation of mesostructure by the turbulent mixing by ice keels as suggested by Corse (1974) is probably a doubtful mechanism due to the lack of evidence of mixing farther under the ice.

The area near the ice margin was characterized by large temperature gradients along isopycnals and by the irregularity and tilting of the isopycnals. These irregularities and tilting must result in lateral pressure gradients that evidently are balanced by complex dynamic flows in the marginal area.

Further investigation led to the discovery of a dynamic hill which extended about 30 km across the margin. The hill was due to the melting process and was notable to a depth of about 10 m. It was interesting that the dynamic hills

were about the same height as the depression computed by Neshyba (1974) for the freezing process. If his numbers are correct, the dynamic hill for the melting case should be many times larger since melting occurred much more rapidly than freezing and was concentrated over a much narrower width. However, it appears that fresh water was lost from the area by circulation, thus greatly diminishing the freshening effect.

The magnitude of the dynamic hill was found to be of lesser importance than the gradient of the hill near the ice margin. The lateral pressure gradient which resulted from the horizontal gradient in dynamic height was assumed to be balanced by internal frictional stresses, and when approximate calculations of the effect of this balance were made, a velocity shear at the surface resulted. This velocity shear was applied to a simple velocity profile which resulted in a deepening of the flow axis and an acceleration of the flow at depth. This result provides a plausible explanation for the source of the downward mixing that is observed at the margins. This hypothesis is also supported by the correlation of larger horizontal dynamic gradients at the surface with a greater sloping of the deep isopycnals and the presence of more severe deep mesostructure. The greater dynamic forces at the surface should result in larger velocity shears and thus stronger effects at depth.

Shallow and deep mesostructure are believed to be related to different degrees of mixing action. Shallow

structure was correlated with the presence of the nose feature while deep structure was related to large dynamic slopes. Deep structure was usually within the density zone of 26.0-26.5 sigma-t units which was found below 20 m depth. The deep structure was located in the vertically broadened areas of this density zone. The low density gradient of this broadened area implies mixing processes, which one might expect from the large gradients in dynamic height. This area of low vertical density gradient also was one where interleaving might easily occur due to the small amounts of energy required to lift a parcel of water. Deep structure appeared to be more severe when the nose feature was not well defined. Thus it would appear that the higher dynamic slopes at the surface cause more severe velocity shears. The resulting stronger mixing effects can destroy the nose feature and thus explain the usual absence of the nose when deep structure is strong.

Shallow mesostructure was related to the nose feature and was generally found above the 26.0 sigma-t contour and thus usually shallower than 20 m depth. It was observed at the boundaries of the nose feature where water types of similar density and different temperatures were available to interleave. Shallow structure, with two exceptions, was found to be more severe in the cases in which deep structure was weak or absent.

B. RECOMMENDATIONS FOR FUTURE INVESTIGATIONS

As a result of this study it is evident that additional data are necessary in future investigations. The probable variations in local flows near the ice margin make it apparent that current vector data are needed for the stations taken near the margins. Data also need to be collected farther into the ice and more exact data on ice concentration and thickness would be helpful. Time series data on the STD parameters and currents, taken simultaneously, would also be useful in determining the time variance of the phenomena.

APPENDIX A

STD DATA FOR STATIONS ANALYZED

The data for each station of the ice crossings analyzed follows. Four stations appear on each page and the respective station number appears in the lower part of each plot. The scales for the horizontal axes are located at the top of each column and the symbols are as follows:

ST, sigma-t

SV, sound velocity (m sec^{-1})

S, salinity (°/₀₀)

T, temperature (°C)

The symbol for each of the above parameters is at the bottom of each trace and an S, T, or V (salinity, temperature, or sound velocity) appears at the top to help distinguish individual traces. The gap usually located at about 10 depth on each trace is due to the requirement for two lowerings of the STD.

MIZPAC 74 STD STATIONS
MG/CC
M/SEC
P.P.T.
DEG C
SE
SU
ST
T
DEPTH (M)
0
70
17
1430
24
-2
22
1455
29
3
27
1480
34
8
S ST
SU
T
22
23
24
25

MIZPAC 74 STD STATIONS
MG/CC
M/SEC
P.P.T.
DEG C
ST
SU
T
DEPTH (M)
17
1430
24
-2
22
1455
29
3
27
1460
+34
8
27
1460
34
9
S ST
SU
T
26
27
28
29

MIZPAC 74 STD STATIONS
MG/CC
M/SEC
P.P.T.
DEG C
ST 17 1430 24 -2
SU 22 1455 29 3
SS 27 1480 34 8
T
SU
SS
30
31
32
33
0
20
DEPTH (M)

MIZPAC 74 STD STATIONS
MG/CC
M/SEC
P.P.T.
DEG C
ST
SU
T
S
DEPTH (M)
0
20
35
37
34
36

MIZPAC 74 STD STATIONS
DEPTH (M)
ST
SU
SI
17
1430
22
-2
22
1455
29
3
27
1480
34
8
39
38
42
40
S
T
SU
0
70

MIZPAC 74 STD STATIONS
MG/CC
M/SEC
P.P.T.
DEG C
ST 17 1430 -2 24 3 22 1455 29 3 22 1480 34 8
SU 17 1430 -2 24 3 22 1455 29 3 22 1480 34 8
T- 17 1430 -2 24 3 22 1455 29 3 22 1480 34 8
S ST
SU
T
13
14
15
16
0
70
DEPTH (M)

MIZPAC 74 STD STATIONS
MG/CC
M/SEC
P.P.T.
DEG C
ST
SU
T
S ST
DEPTH (M)
47
48
49
50
17 1430 24 -2
22 1455 29 3
27 1480 34 8
0
20

MIZPAC 74 STD STATIONS
MG/CC
M/SEC
P.P.T.
DEG C
ST 17 1430 24 -2
SU 22 1455 29 3
S T 27 1430 34 8
DEPTH (M)
0
20
51
52
53
54
S ST
SU
T

MIZPAC 74 STD STATIONS
MG/CC
M/SEC
P.P.T.
DEG C
27
1480
34
8
22
1455
29
3
17
1430
24
-2
S
SU
T
56
58
55
52
0
20
DEPTH (M)

MIZPAC 74 STD STATIONS
MG/CC
M/SEC
P.P.T.
DEG C
SST
SU
T
59
60
61
62
DEPTH (M)

MIZPAC 74 STD STATIONS
MG/CC
M/SEC
P.P.T.
DEG C
27
1480
34
0
22
1455
29
3
17
1430
24
-2
ST
SU
T
S ST
SU
T
64
66
63
65
0
20
DEPTH (M)

MIZPAC 74 STD STATIONS
MG/CC
M/SEC
P.S.U.
DEG C
27
1480
34
8
22
1455
29
3
17
1430
24
-2
SST
SU
T
68
70
67
69
0
200
DEPTH (M)

MIZPAC 74 STD STATIONS
MG/CC
M/SEC
P.P.T.
DEG C
22
1480
34
8
22
1455
29
3
17
1430
24
-2
SST
SU
T
SV
72
74
71
73
0
20
DEPTH (M)

MIZPAC 74 STD STATIONS
MG/CC
M/SEC
P.P.T.
DEG C
DEPTH (M)
ST
SV
T
12
1430
24
-2
22
1455
29
3
22
1480
34
8
17
1430
24
-2
22
1455
29
3
22
1480
34
8
SST
SV
T
90
91
92
93
0
70

MIZPAC 74 STD STATIONS
MG/CC
M/SEC
F.P.T.
DEG C
17 1430 24 -2
22 1455 29 3
22 1480 34 8
22 1480 34 6
95
94
97
96
S
ST
SU
T
DEPTH (M)
0
20

MIZPAC 74 STD STATIONS
MG/CC
M/SEC
F.P.T.
DEG C
ST 12 1430 22 1455 22 1480 22 1980 12
SU 24 29 34 33
ST -2 3 8 8
98
99
100
101
SU
ST
T
0
70
DEPTH (M)

MIZPAC 74 STD STATIONS
MG/CC
M/SEC
DEG C
DEPTH (M)
SSH
SU
T
102
103
104
105
0
20

MIZPAC 74 STD STATIONS
MG/CC
M/SEC
P.P.T.
DEG C
ST 17 22 27
SU 1430 1455 1480
SS 24 29 34
T -2 3 8
0
70
DEPTH (M)
SST
SU
T
106
107
108
109

MIZPAC 74 STD STATIONS

BIBLIOGRAPHY

Applied Physics Laboratory Report APL-UW 7223, Studies in the Marginal Ice Zone of the Chukchi and Beaufort Seas. A Report on Project MIZPAC-71B, by G. R. Garrison and E. A. Pence, 110 p., 31 January 1973.

Campbell, W. J., "The Wind-Driven Circulation of Ice and Water in a Polar Ocean," J. Geophys. Res., v. 70, no. 14, p. 3279-3301, 15 July 1965.

Corse, W. R., An Oceanographic Investigation of Mesostructure near Arctic Ice Margins, Master's Thesis, Naval Postgraduate School, Monterey, California, 1974.

McLellan, H. J., Elements of Physical Oceanography, p. 74-79, Pergamon Press, 1965.

Naval Postgraduate School Report NPS-58PA73121A, Oceanographic Measurements near the Arctic Ice Margins, by R. G. Paquette and R. H. Bourke, 96 p., December 1973.

Neshyba, S. and Badom-Dangon, A., "On Ocean Current Induced by a Prograding Ice Pack," Geophys. Res. Papers, v. 1, no. 8, p. 351-354, December 1974.

Neuman, G. and Pierson, W. J., Principles of Physical Oceanography, p. 211-212, Prentice-Hall, Inc., 1966.

Oceanographic Prediction Division, U.S. Naval Oceanographic Office, Manual of Short-Term Sea Ice Forecasting, by W. I. Wittman and G. P. MacDowell, p. 59, July 1963.

Paquette, R. G. and Bourke, R. H., "Observations of the Coastal Current of Northwestern Alaska," J. Mar. Res., v. 32, no. 2, p. 195-207, 15 May 1974.

Paquette, R. G., Bourke, R. H., and Corse, W. R., The Source of Temperature Mesostructure in the Ocean near the Arctic Ice Margin, paper presented at Fall Annual Meeting, American Geophys. Union, San Francisco, California, December 1974.

INITIAL DISTRIBUTION LIST

		No. Copies
1.	Defense Documentation Center Cameron Station Alexandria, Virginia 22314	2
2.	Library, Code 0212 Naval Postgraduate School Monterey, California 93940	2
3.	Department Chairman, Code 58 Department of Oceanography Naval Postgraduate School Monterey, California 93940	3
4.	Assoc Professor R. G. Paquette, Code 58 Pq Department of Oceanography Naval Postgraduate School Monterey, California 93940	3
5.	Oceanographer of the Navy Hoffman Building No. 2 200 Stovall Street Alexandria, Virginia 22332	1
6.	Office of Naval Research Code 480 Arlington, Virginia 22217	1
7.	Dr. Robert E. Stevenson Scientific Liaison Office, ONR Scripps Institution of Oceanography La Jolla, California 92037	1
8.	Library, Code 3330 Naval Oceanographic Office Washington, D. C. 20373	1
9.	SIO Library University of California, San Diego P. O. Box 2367 La Jolla, California 92037	1
10.	Department of Oceanography Library University of Washington Seattle, Washington 98105	1

11.	Department of Oceanography Library Oregon State University Corvallis, Oregon 97331	1
12.	Commanding Officer Fleet Numerical Weather Central Monterey, California 93940	1
13.	Commanding Officer Environmental Prediction Research Facility Monterey, California 93940	1
14.	Department of the Navy Commander Oceanographic System Pacific Box 1390 FPO San Francisco 96610	1
15.	Commander Naval Weather Service Command Washington Navy Yard Washington, D. C. 20390	1
16.	Dr. R. H. Bourke, Code 58 Bf Department of Oceanography Naval Postgraduate School Monterey, California 93940	2
17.	Dr. Waldo K. Lyon Director, Arctic Submarine Laboratory Naval Undersea Center San Diego, California 92132	2
18.	LT Allan E. Karrer, USN USS INDEPENDENCE (CV-62) FPO New York 09501	2